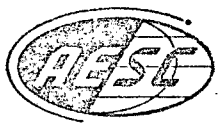

LWS DESIGN REPLACEMENT STUDY

FINAL REPORT
OPTIMUM DESIGN AND TRADEOFF ANALYSIS

CONTRACT NAS 9-13189

PREPARED FOR

NATIONAL AERONAUTICS SPACE ADMINISTRATION
MANNED SPACECRAFT CENTER
HOUSTON, TEXAS

REPORT NO. 4713

23 FEBRUARY 1973

AEROJET
ELECTROSYSTEMS
COMPANY

LWS DESIGN REPLACEMENT STUDY

FINAL REPORT

OPTIMUM DESIGN AND TRADEOFF ANALYSIS

Contract NAS 9-13189

Prepared for

NATIONAL AERONAUTICS SPACE ADMINISTRATION
MANNED SPACECRAFT CENTER
HOUSTON, TEXAS

Report No. 4713

23 February 1973

AEROJET ELECTROSYSTEMS COMPANY
A DIVISION OF AEROJET-GENERAL
1100 WEST HOLLYVALE STREET, AZUSA, CALIFORNIA 91702

II

Report No. 4713

TABLE OF CONTENTS

LIST OF FIGURES

LIST OF TABLES

1. INTRODUCTION

Under National Aeronautics and Space Administration Contract NAS 9-13189, Aerojet ElectroSystems Company has performed a study to generate and demonstrate a design for two long-wavelength (LW) focal-plane and cooler assemblies, including associated preamplifiers and post-amplifiers. The focal-planes and associated electronic assemblies are intended as direct replacement hardware to be installed into the existing 24-channel multispectral scanner used with the NASA Earth Observations Aircraft Program. An organization skilled in the art of LWIR systems can fabricate and deliver the two long-wavelength focal-plane assemblies described in this report when provided with the data and drawings developed during the performance of this contract.

The intent of this report is to discuss the concepts developed during the study including the alternative approaches and selection of components. Modifications to the preliminary design as reported in a Preliminary Design Review meeting at the NASA Manned Spacecraft Center have also been included.

The purpose of the study was to produce a demonstratable replacement design for arrays 3 and 4, which operate in the 2.1 through 4.75 μm and 6.0 through 13.0 μm spectral regions, respectively. On 29 January 1973, the validity of the selected design was demonstrated for each of the two arrays using breadboard type hardware. Documentation has been prepared in sufficient detail to allow production of the flight hardware (see drawing list, Tables I and II). This hardware design will interface with the Multispectral Scanner System in the same positions as present Arrays 3 and 4 as shown on Figure 1. These units will meet the performance requirements of the Statement of Work as included in the NASA RFP 9-BB-321-57-3-12P. The predicted performance of the design has been demonstrated during this study program using one typical channel from each array.

Various alternate concepts were analyzed and the optimum concepts selected. Criteria used in selection of optimum design concepts were:

TABLE I - Array #3 Drawing List

Drawing No.	Title	Quantity Req'd
1301000	Focal Plane/Cryocooler Assy.	-
1301001-1	Housing - Cold Finger	1
1301002	Adapter - Cooler	1
1301003	Base - Rotational Adjustment	1
1301004	Screw - Adjustment	2
1301005	Shaft Lateral Adjustment	2
1301006	Nut - Rotational Adjustment	1
1301007	Screw - Rotational Adjustment	1
1301008	Base - Lateral Adjustment	1
1301009	Base - Horizontal Adjustment	1
1301010	Table - Horizontal Adjustment	1
1301011	Shaft - Horizontal Adjustment	2
1301013	Plate - Vertical Adjustment	1
1301015	Heat Sink Envelope	1
1301018	Window - Sapphire	1
1301019	Housing - Focal Plane	1
1301020	Schematic Ass'y - Focal Plane/Cryocooler	-
1301022	Cold Stop	1
1301024	Isolator-Cold Finger	1
1301026	Heat Sink - Master	1
1301027	Heat Sink - Detector Element #13	1
1301028	Heat Sink - Detector Element #14	1
1301029	Heat Sink - Detector Element #15	1
1301030	Focal Plane - Multispectral	-
1301031	Tape Cable (Signal)	1
1301033	Support Bracket - Preamp.	1
1301041	Filter - Spectral	3
1301043	Support Plate - Filter #13	2
1301044	Support Plate - Filter #14	2
1301045	Support Plate - Filter #15	2
1301046	Frame - Window Retaining	1
1301047	Tape Cable - Heater/Sensor	1
1300076	Sleeve - Insulating	6

[illegible] - Array #4 Drawing List

Drawing No.	Title	Quantity Req'd
[illegible]	Ass'y - Basic Layout	-
1300999	[illegible] old Finger	1
1301001-2	[illegible] ional Adjustment	1
1301003	[illegible] stment	2
1301004	[illegible] eral Adjustment	2
1301005	[illegible] ional Adjustment	1
1301006	[illegible] ional Adjustment	1
1301007	[illegible] al Adjustment	1
1301008	[illegible] ontal Adjustment	1
1301009	[illegible] zontal Adjustment	1
1301010	[illegible] zontal Adjustment	2
1301011	[illegible] ooler	1
1301012	[illegible] ical Adjustment	1
1301013	[illegible] velope	1
1301014	[illegible] cal Plane	1
1301016	[illegible] manium	1
1301017	[illegible] s'y - Focal Plane/Cryocooler	-
1301020	[illegible] Master	1
1301021	[illegible]	1
1301023	[illegible] old Finger	1
1301025	[illegible] et - Preamp	1
1301032	[illegible] Clamp	1
1301034	[illegible] pe Cable	1
1301035	[illegible] ng Board	1
1301036	[illegible] agram - Buffer Amplifier	-
1301037	[illegible] op Assembly	1
1301038	[illegible] ng Board - Heater/Sensor	1
1301039	[illegible] - Multispectral	-
1301040	[illegible] pectral	7
1301042	[illegible] - Heater/Sensor	1
1301047	[illegible] - Signal	1
1301048		

Drawing No.	Title	Quantity Req'd
1301050	Focal Plane/Cryocooler Layout	-
1300066	Frame - Window Retaining	1
1300075	Frame - Spectral Filter	1
1300076	Sleeve - Insulating	6
1300355	Heat Sink - Det. Element #16	1
1300356	Heat Sink - Det. Elements #17, 18, 19 & 20	1
1300357	Heat Sink - Det. Element #21	1
1300358	Heat Sink - Det. Element #22	1

a. Performance: The performance of arrays 3 and 4 must be equal to or better than the requirements specified in the Statement of Work. However, since the requirements of the system are within the realm of presently available technology and materials, the trade-studies were limited to examination of items and techniques with demonstrated performance in similar applications.

b. Reliability: Only those components, materials and equipment with demonstrated reliability in similar applications were considered. The use of unproved designs and materials, no matter how attractive the claims, does not appear to be justifiable based on the schedule considerations and the need for long-term,trouble-free performance of these elements of the system.

c. Field Maintainability: The need to achieve ease of maintenance, commonality of parts and equipment, location of components outside of the evacuated space where possible, easily accessable valving for system evacuation, and accessable adjustments for positioning, alignment and electrical adjustment were all considered during the evaluation of the design concept.

d. Technical Risk, Schedule and Cost: Aerojet ElectroSystems Company considers the system concepts presented to represent a design which:

- Has minimal technical risk.
- Can be developed and manufactured in a reasonable time without excessive basic research.
- Requires minimum development and manufacturing costs.

e. Commonality and Interchangeability of Components: Array 4 has been designed to use the identical detector focal plane, filter, and window assemblies as are presently used with the Array 4 now in use. Thus, these

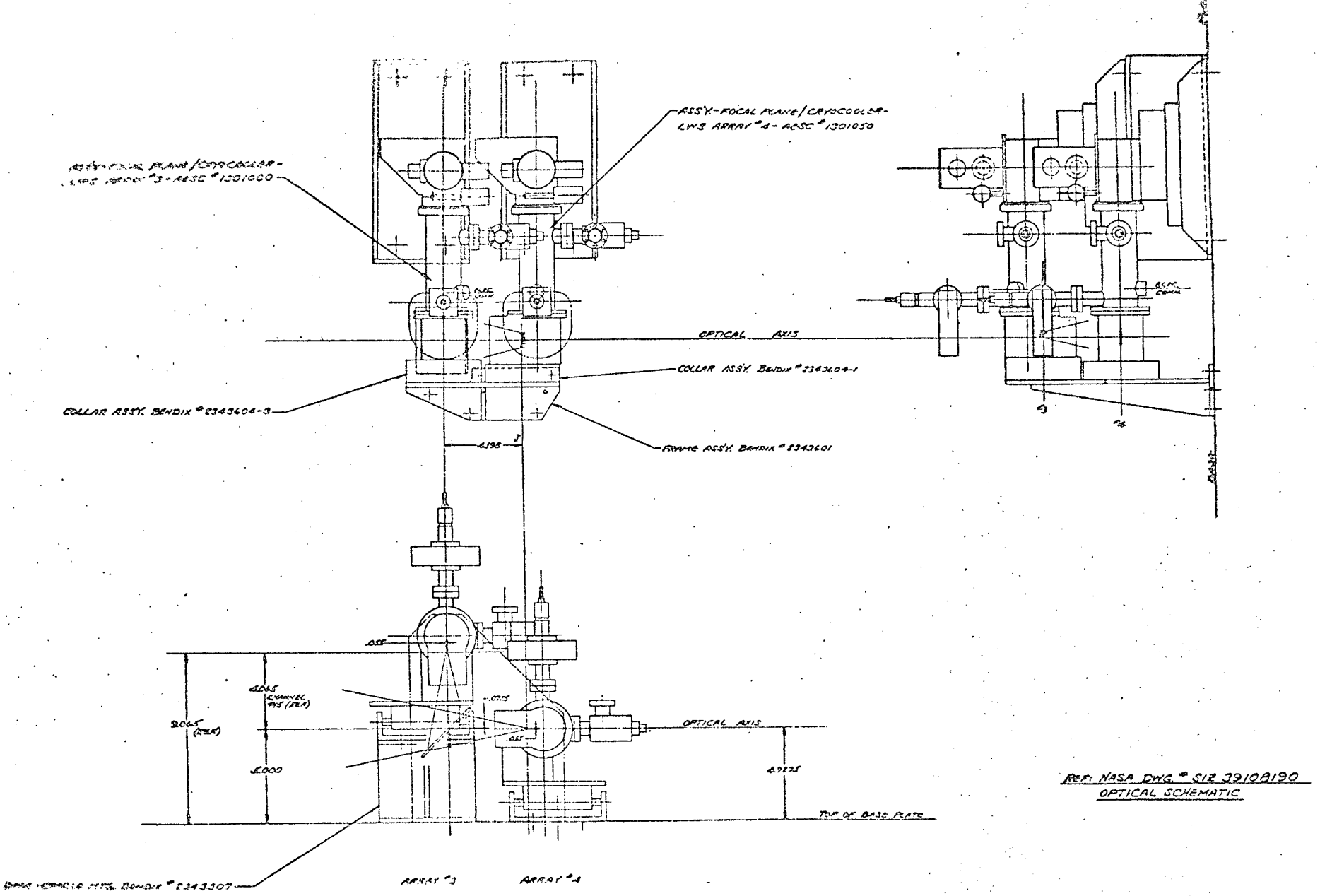

REF: NASA DWG. # SIR 3910B190
OPTICAL SCHEMATIC

FIGURE 1. - INTEGRATED ASSEMBLY, FOCAL PLANE/CRYOCOOLER, LWS No. 3 AND 4

FOLDOUT FRAME 1

FOLDOUT FRAME 2

items can be used as direct replacement spares with the current design. In addition, the cooler equipment for the current design, with minor exception, is directly interchangeable with systems currently in use by MSC. Thus, spare part provisioning and program cost will be reduced.

2. DESIGN DESCRIPTION

The optimum design presented for arrays 3 and 4 is capable of furnishing the specified performance and incorporates features which make it attractive in terms of reliability and maintainability in the field. The arrays can be built using available technology and materials.

2.1 Detectors

Detector materials selected are indium antimonide (InSb) for array 3 and Mercury-doped germanium (Ge:Hg) for array 4. The detectors will be cold shielded and spectrally filtered in accordance with the Detector/Filter requirements of Table III. These requirements were originally included in NASA RFP 9-BB-321-57-3-12P and remain valid after review and analysis of system requirements.

2.2 Refrigerator

A Gifford McMahon type closed cycle refrigerator unit has been specified for the design. The unit selected is manufactured by Cryogenic Technology, Inc., an affiliate of A. D. Little, Inc., and is designed as their cryodyne Model 0120. For cost-effectiveness, the array housings and master heat sinks have been configured such that the coolers required are identical to units already in use by NASA at MSC. Thus, most of the cooler equipment required for the replacement arrays is presently available at MSC. The exception to this general statement is a dummy second stage displacer unit which is required for array 3.

The cooler is comprised of two sections. The first, refrigerator section, includes the 77°K and 27°K stages, and a valving system driven by a motor and a scotch yoke drive assembly. The second unit, a compressor, can be mounted at a remote location from the refrigerator (and cold head) section. The two sections of the assembly are connected with flexible hoses.

TABLE III

Detector/Filter Requirements

1	2	3	4	5	6	7	8
ARRAY	CHANNEL	CENTER WAVELENGTH MICRONS	BAND LIMITS 50 PERCENT POINTS	DETECTOR SENSITIVE AREAS ± 0.0005	$D^*(\lambda, 1000, 1)$ Cm $\sqrt{Hz}/W$	RESPONSE BANDWIDTH (MHz)	FOV
3	13	2.23	±0.13	0.087 X 0.055	3 X 10"	0.5	f/1.4
3	14	3.77	±0.23	0.102 X 0.055	3 X 10"	0.5	f/1.4
3	15	4.63	±0.125	0.055 X 0.055	3 X 10"	0.5	f/1.4
4	16	6.50	±0.50	0.111 X 0.055	4×10^{10}	0.5	f/1.4
4	17	8.55	±0.25	0.055 X 0.055	4×10^{10}	0.5	f/1.4
4	18	9.05	±0.25	0.055 X 0.055	4×10^{10}	0.5	f/1.3
4	19	9.55	±0.25	0.055 X 0.055	4×10^{10}	0.5	f/1.3
4	20	10.55	±0.45	0.100 X 0.055	4×10^{10}	0.5	f/1.3
4	21	11.50	±0.50	0.111 X 0.055	4×10^{10}	0.5	f/1.4
4	22	12.50	±0.50	0.111 X 0.055	4.5×10^{10}	0.5	f/1.4

NOTE: AS A DESIGN GOAL, D_λ^* SHALL BE AS IN COLUMN 6 FOR ALL FREQUENCIES FROM 200 Hz TO 0.5 MHz AND FOR FREQUENCIES LESS THAN 200 Hz DOWN TO 6 Hz, D_λ^* SHALL NOT DECREASE FASTER THAN BEING PROPORTIONAL TO FREQUENCY.

Although the required operating temperature for InSb and Ge:Hg detectors are different (77°K and 27°K, respectively), the same basic cooler is specified and is capable of meeting the requirements of both arrays. In the 77°K application, array 3, a "dummy" second stage displacer is substituted. This dummy stage is specified because focal plane temperature control at 50° above the nominal cold finger temperature of 27°K to the required 77°K would require excessive heat input. However, the compressors required for both systems are identical. This commonality is practical since the slight additional weight and power consumption are not critical for this application.

The model 0120 has a capacity of 1 to 1.5 watts at 27°K which is sufficient for operation of either focal plane assembly. At either focal plane temperature, Aerojet considers active temperature control necessary. Active proportional temperature control (see Section 2.6) has been included in the design. In addition to the active temperature control system, a passive temperature damping device is required to reduce thermal "chugging," a characteristic of this refrigeration system. The "chugging," if not compensated, would result in temperature variations at the heat sink of the order of 1° occuring at a frequency of approximately 2.6 cycles per second. The manufacturer recommends installation of a special metal alloy thermal capacitor between the refrigerator load (focal plane assembly) and the cold finger. This thermal capacitor is a special lead-tin alloy which functions as a low pass thermal filter. It is estimated that a thickness of up to 1/4 inch will be required to achieve the desired short term temperature stability of less than 0.01°K. The shim thickness must be determined experimentally as analytical methods are not presently available. However, the manufacturer claims that the selection is not difficult. The mechanical design for the focal plane/cooler assembly provides adjustment to compensate for the shift in focal plane position resulting from installation of the filter. Mounting of the arrays has been designed such that the complete refrigeration system may be removed from the MSS without disturbing the array alignment. This feature will facilitate maintenance of the cooler subsystem.

A typical compressor unit occupies a volume of approximately 10.5 x 10.5 x 8.75 inches; weighs 11 pounds, and uses 750 watts of three phase 400 cycle power. The refrigeration unit weighs 4.5 pounds and uses 40 watts of power. The coolers have an MTBF greater than 1,000 hours and meet the requirements of MIL-E-5400. Because of the commonality of cooler requirements

between this program and other devices used at MSC, it will be possible to use existing compressors, flexible connecting lines, adsorbers and refrigeration units. Modification of the displacer cylinders to receive the array 3 and 4 cold stations and the substitution of the dummy stage for array 3 can be coordinated with NASA MSC. For this reason, detailed requirements and mounting drawings have not been included in this study. However, the compressor unit connects to the refrigeration assemblies with flexible hoses so that no particular difficulty will be encountered with the installation in the MSS.

2.3 Preamplifier/Post-Amplifier

The recommended approach for detector preamplifiers and post-amplifiers remains essentially as outlined in the AESC proposal, PN8837-05-23. The concept of a transimpedance preamplifier followed by a post amplifier incorporating the dc restoration feature has been retained.

An impedance reducing device operating at cryogenic temperatures will be situated in close proximity to the detector. (The device will be a MOSFET (Siliconix G118F or M511) for the Ge:Hg detectors of array 4 and a JFET 2N5199 for the InSb detectors of array 3). Detector load resistors will also be located near the associated detector and maintained at the focal plane temperature to reduce lead capacitance and reduce the thermal noise generated by the load resistor. This approach virtually eliminates RC roll-off problems, minimizes the possibility of microphonic pick-up and simplifies testing procedures.

2.4 Vacuum Enclosure

The vacuum enclosure has been designed with only five interfaces requiring seals and are located as follows:

a. Cold-finger housing to refrigerator.
b. Window to focal-plane housing.
c. Cold-finger housing to focal plane housing.
d. VacIon* pump to cold-finger housing.
e. Roughing valve to cold-finger housing.

*VacIon Pump is a registered name and the pump is manufactured by Varian Vacuum Division, Palo Alto, Calif.

The application of crushable metal seals at these interfaces as discussed in the preliminary design review was investigated. Crushable metal seals appear to provide superior vacuum integrity compared to elastomeric sealing materials such as Viton or polyamide. However, application of crushable seals also introduces some problems relating to maintenance of the system, mechanical alignment, and possible distortion of the sealing surfaces. For example, the window to focal-plane housing seal using crushable metal is not recommended because the pressures required to accomplish the seal could fracture the germanium window material. For this interface, the window frame and O-ring seal used with the present array has been retained to permit interchangeable windows for the two systems. Use of metal-to-metal seals for the VacIon pump and roughing valve connections presents no difficulty, and the use of Mini-ConFlat flanges* has been specified. An O-ring type seal has been specified for the refrigerator to cold-finger housing seal and the focal-plane housing to cold-finger housing interfaces. This selection was based on the alignment considerations, and on the additional cost impact of the seal development using crushable metal seals that would be compatible with this design. Since the VacIon pumps have been retained and because the window of the existing array 4 should be interchangeable with the present design, the development of special seals does not appear to be cost effective. Materials used within the evacuated space were selected to minimize outgassing. In this regard, the Aerojet proposal suggested that the preamplifier would be located within the Dewar. Consideration of possible problems with outgassing of the various electronic elements dictates that the preamplifier be mounted outside of the Dewar since the FET impedance reduction permits this change with minimal penalty due to lead capacity, etc. The selected design specifies this configuration.

NASA indicated during the design review meeting that they have been experiencing difficulty with long pump-down times; in part caused by the relatively small porting of the Cyrolab mini-valve and also due to slow roughing pump evacuation. To eliminate these problems, a Zeolite cryogenic type

*Varian Vacuum Division, Palo Also, Calif.

roughing pump system is suggested, and a larger-ported vacuum valve (Varian 3/4 in. full-flow, all-metal valve, part No. 951-5015) has been included in the design.

2.5 Mechanical Focal Plane/Cryodyne Assembly

The mechanical design places the detectors at the prescribed position relative to the existing dichroic mirror when array 4 is mounted to the baseplate and array 3 is mounted to the existing I-beam support. Layouts of the two assemblies are included as Figures 2 and 3 while their relative location in the MSS is shown in Figure 1.

Translation adjustment of approximately $\pm$ 1/4 inch in the X, Y, and Z directions and focal plane rotational adjustment of $\pm$ 5° is provided. Compensation for thermal damper installation will be accomplished with shims and will not reduce the above adjustments. Adjustment in the X, Y and rotational directions uses lead-screws to establish position and additional screws to lock the final position. The Z direction adjustment uses pairs of jack screws and locking screws. The large range of adjustment has been included in the design to prevent stressing the structures when attaching to the scanner baseplate (or I-beam) and adapter flange. An adjustable adapter flange will also be provided so that once the unit is aligned in position, the flange end can then be secured without introduction of stress on the unit. The mechanical package for the arrays is compatible with the existing structural interfaces and allows the existing shroud to be used.

The envelope of the replacement arrays is considerably smaller than the arrays being replaced due to the smaller dimensions of the refrigerator portion of the coolers. See Figure 4. The compressor section has been designed for remote installation using flexible hoses.

2.6 Focal Plane Temperature Control

As mentioned earlier, a long term temperature control system for the focal plane assembly is necessary to obtain optimum performance from the detectors. The temperature variation should be maintained at less than $\pm$ 3°K for the InSb detector (operating at nominally 77°K) and less than $\pm$ 2°K for the Ge:Hg detector (operating at nominally 27°K). The temperature control system will limit the temperature excursion to $\pm$ 0.5°K.

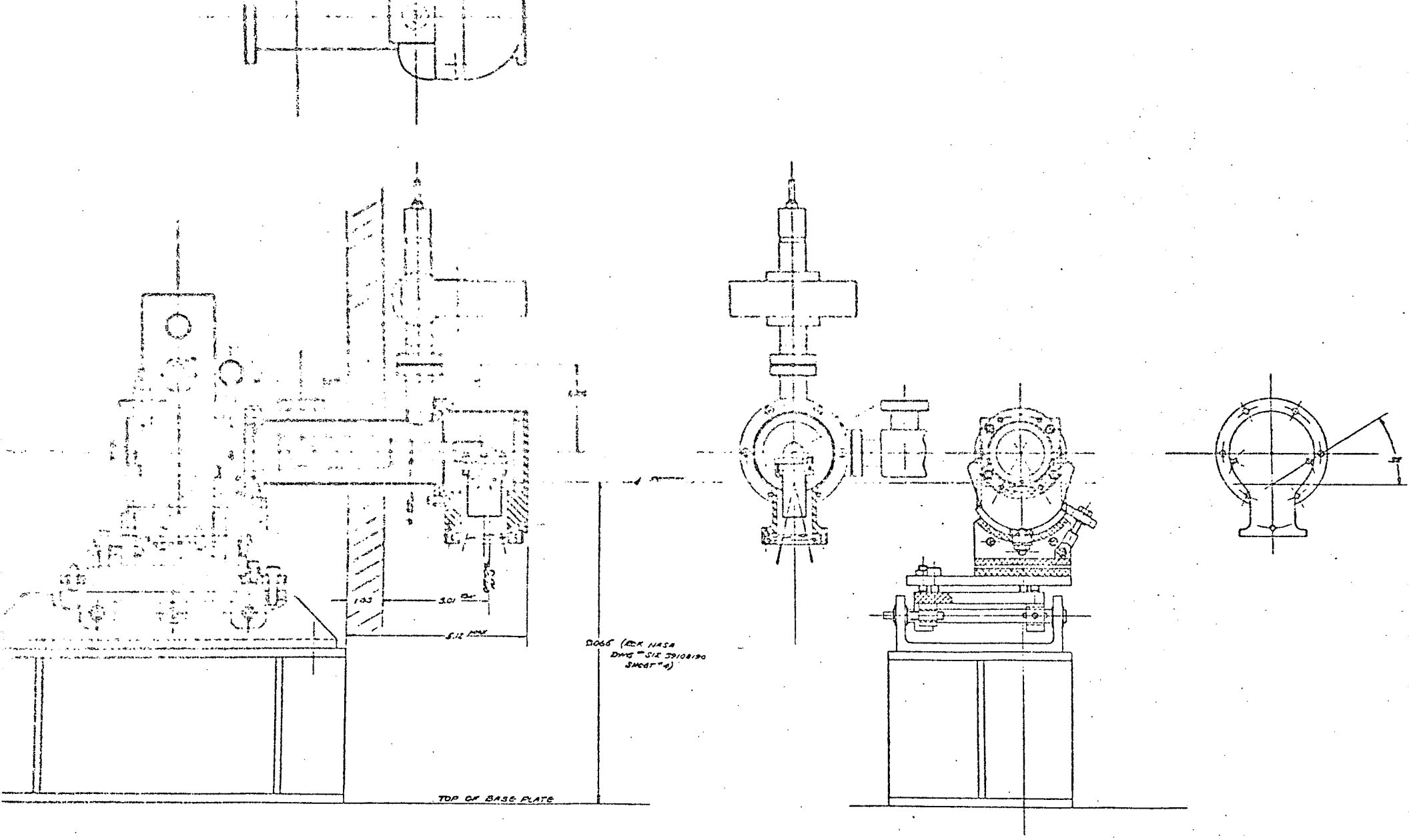

Figure 2. - ASSEMBLY, FOCAL PLANE/CRYOCOOLER, LWS InSb ARRAY #3

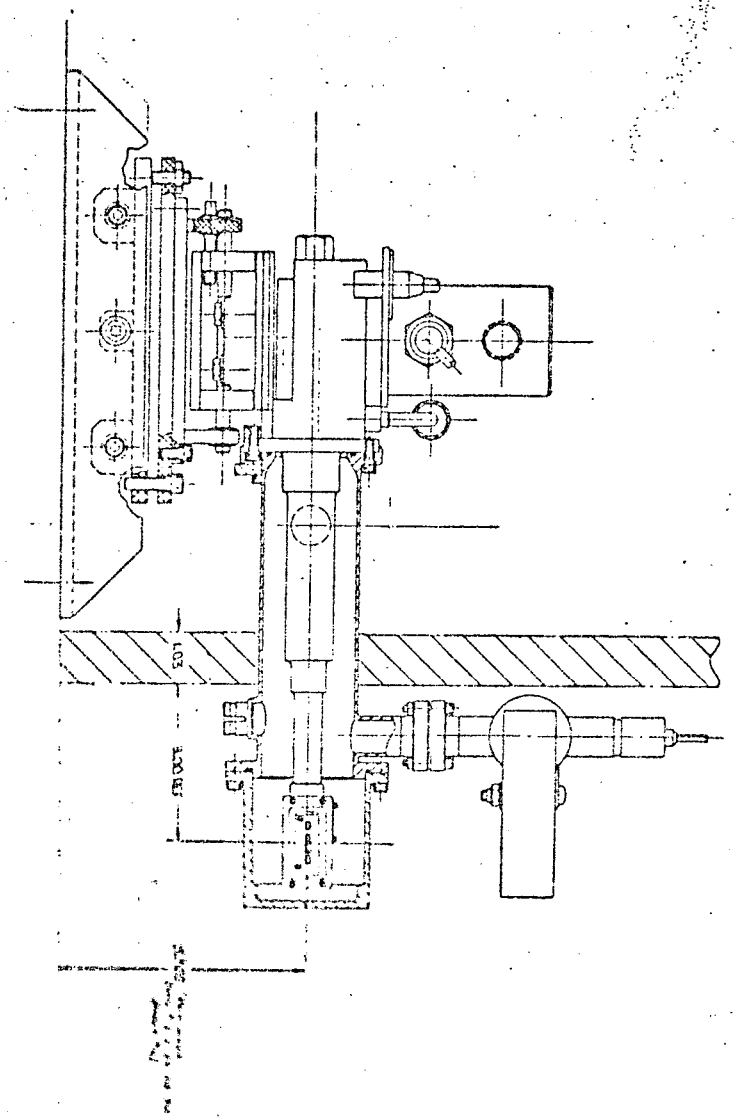

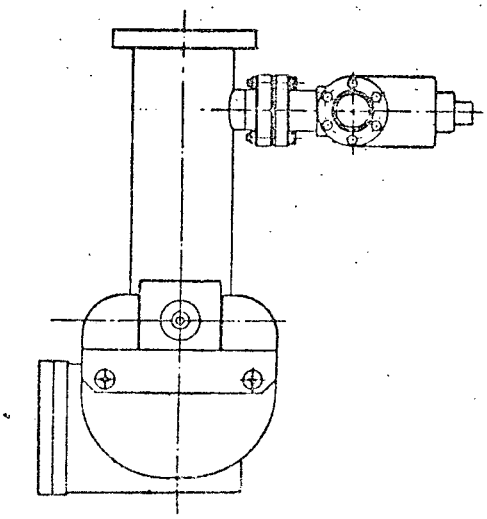

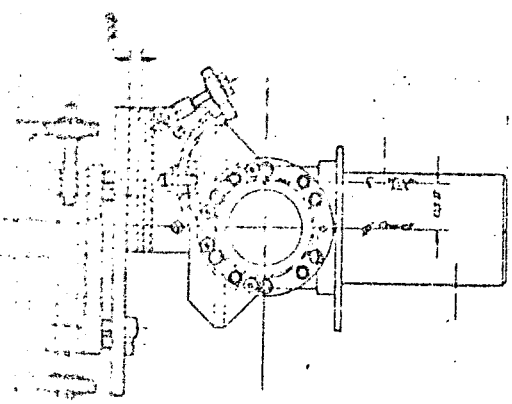

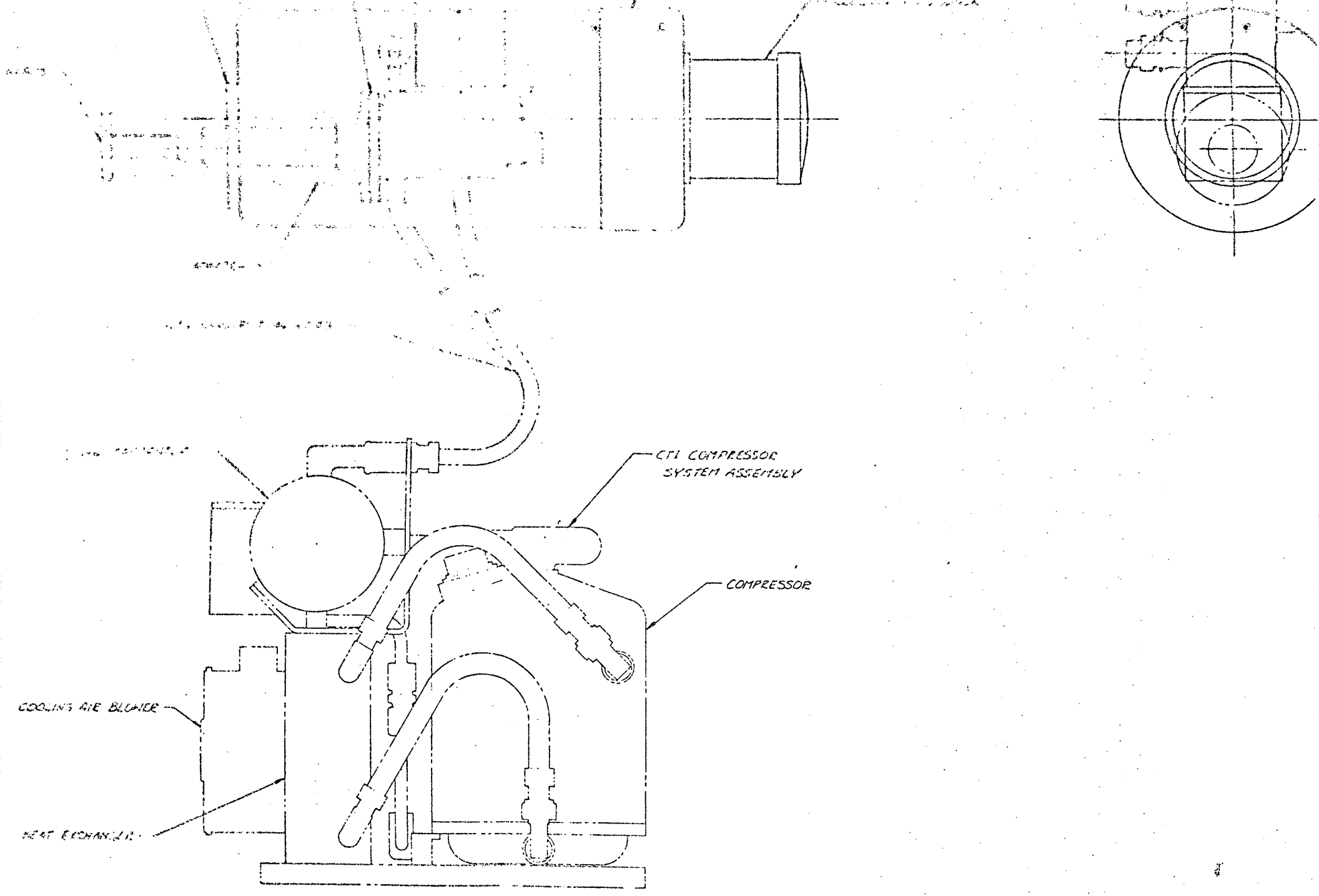

FIGURE 4. - COOLER COMPARISON, MARINER VIIC/CTI C120

FOLDOUT FRAME 1

FOLDOUT FRAME 2

with
revious
table
portion

similar to the unit required for the LWS have been
rojet. Measured performance of these units is
or the present program. A schematic diagram of
oller circuit is included as Figure 5.

emperat
rator
ll not
at th
ight
e cons
value
o thi
mate d
be e
ain th

rol system will operate closed loop and will not
t once the operating set point has been established.
ssary to provide a potentiometer control of
console. Instead, temperature null indicator leads
he circuit to permit installation of a null indi-
s will indicate when the temperature has reached
the control system is operating properly. Although
ill not be linear, it will be possible to estimate
from the desired temperature. Actual temperature
ut this will require adjustment of a potentiometer
onics package (see Figure 5).

ronic
ace
high
r port
refri
plaker
vided
ampli
he po
Hz, 1

or electronics installation (volume approxi-
g by 6" wide) is located directly behind the CTI
e arrays. This space is now available because the
require considerably less space than the presently
(see Figure 4). A separate electronic package
array and will contain the power supply, preampli-
h zero restore and focal plane temperature control
es will operate from either 400 Hz, 115V aircraft
to facilitate laboratory checkout.

cilita
temper
socket
uit com
ds to

checkout the signal conditioning for each channel
ntroller circuits will be installed on individual
used for mounting the operational amplifiers or
Also, rhodium plated contacts have been specified
oblems of contact wear and corrosion.

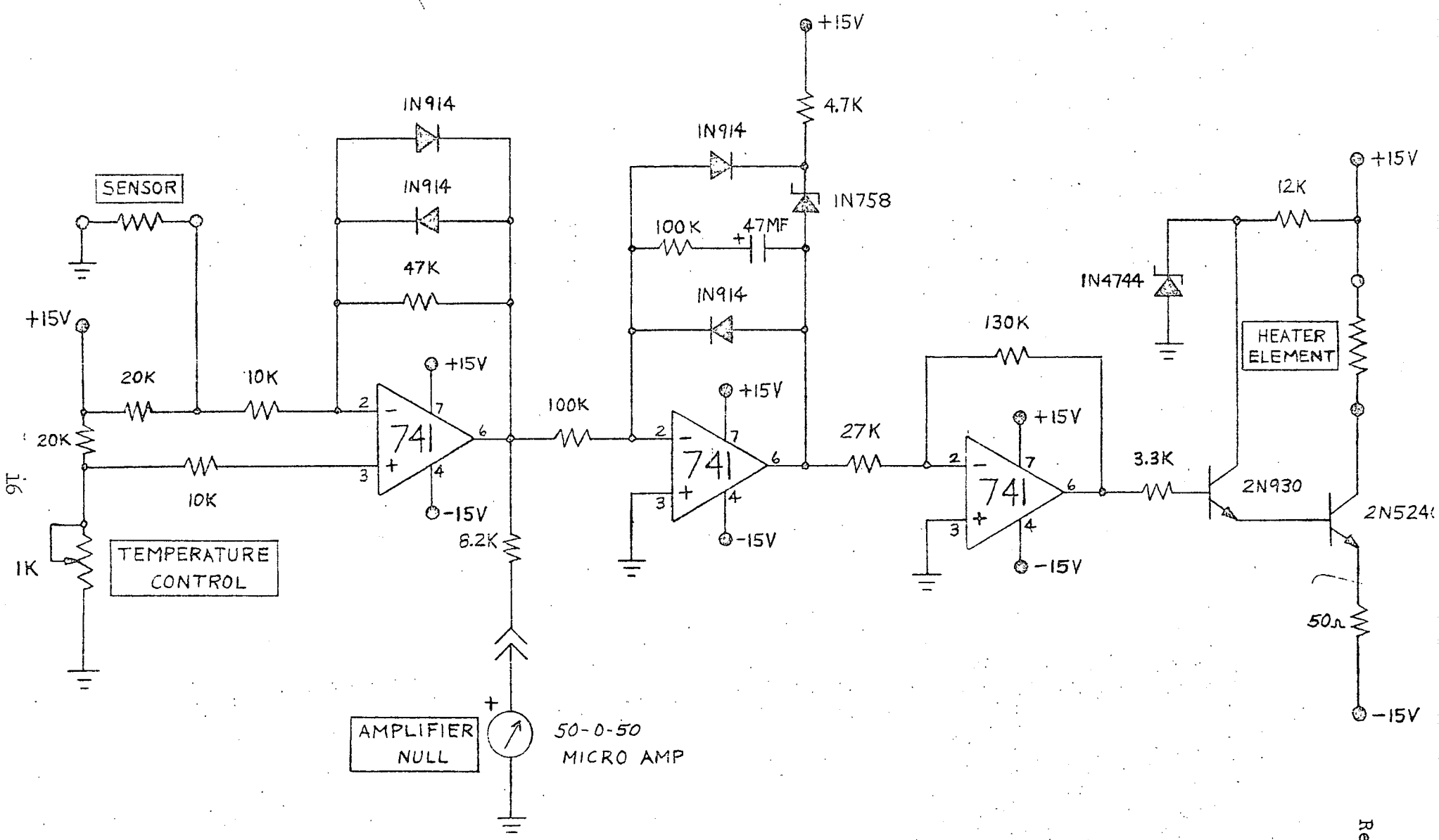

FOCAL PLANE TEMPERATURE CONTROLLER

Figure 5

Report No. 4713

It was reported that severe electrical noise can be present during scanner operation due to the SCR speed control devices used with the scanner drive. To reduce the effect of this noise, the high gain portions of the system electronics will be packaged to minimize the noise pickup through extensive electrostatic shielding, application of ground planes on the printed circuit boards, and single point chassis grounding.

2.8 Electrical Requirements for Interface with the MSS

2.8.1 Frequency Response

The updated frequency response required for operation should be less than 3 db down at frequencies of slightly more than 200 KHz. Since the original requirement specified a flat frequency response to 250 KHz, the circuits have been designed to this value and the revised requirement will be exceeded. The low end of the specified frequency response requirement requires clarification. Originally, NASA RFP 9-BB321-57-3-12P, Paragraph 2.3.3.4.2 specified that the preamplifiers must be dc coupled. The requirement was later revised to mean essentially dc coupled (i.e., a low frequency response of approximately 0.001 Hz). This revision resulted from a determination that zero restoration, using a coupling capacitor in the signal processing chain to permit clamping to the reference signal, was the optimum technique.

Also, analysis of the system requirements indicates that 10 Hz is the lowest sampling rate expected which also supports the ac coupling premise. AC coupling is desirable because dc coupling adds unnecessary complexity to the amplifier section due to dc drifts and the additional requirements of holding very tight tolerances on the preamplifier bias levels. In operation this would mean that considerable adjustment of the preamplifiers would be required to prevent saturation with minor changes in bias. However, it is desirable even with ac coupling, to limit the low frequency response

to the highest value acceptable within the operational requirements of the MSS. If the system is ac coupled with very low frequency capability (to approximate dc coupled condition), it is necessary to provide high gain in the feedback loop and/or additional stages of amplification. This further sensitizes the circuit to bias, temperature, etc. A determination of the actual requirement was made to provide adequate low frequency response without adding unnecessary complexity. A droop of 1% in signal during the scan period was used as a basis for this determination.

Figure 9 shows a low frequency roll of 20 db/decade with a 3 db point of 1.5 Hz. This corresponds to a time constant ($\tau = \frac{\tau}{\omega}$) determined as follows:

$$\omega = 2\pi f = \frac{1}{\tau}$$

$$\tau = \frac{1}{2\pi f} = \frac{0.159}{f}$$

$$= 106 \text{ milliseconds}$$

For a target dwell time of 40° and a minimum scanner rate of 600 rpm, a maximum dwell time is computed as follows:

$$\tau_{\text{dwell max}} = \frac{60 \text{ sec/min}}{600 \text{ rev/min}} \times \frac{40^{\circ}}{360^{\circ}}$$

$$= \frac{100}{9} \text{ ms} = 11.1 \text{ milliseconds}$$

From this, droop is found by the following relationship:

$$\% \text{ droop} = \left(1 - e^{-t/\tau}\right) 100\%$$

$$= \left(1 - e^{-\frac{11.1}{106}}\right) 100\%$$

$$= (0.1)\ 100\% = 10\%$$

Therefore:

$$\% \text{ droop} = \left(1 - e^{-\frac{11.1}{3180}}\right) 100 = 0.348\%$$

which is well within the 1% droop goal. Thus, a low frequency response of 0.05 Hz appears reasonable and practical for the MSS system.

2.8.2 Gain and Offset

The input to the MSS video processor from Arrays 3 and 4 post-amplifiers must not be offset more than 0.25 volts. The gain of the detector/amplifier systems must also be sufficient to provide an output of 1.0 volt for a $40^{\circ}K$ background temperature difference. The 0.25 maximum offset voltage requirement will be met by providing an adjustment on the clamp level circuit or by adjusting the offset control on the final operational amplifier stage. A variable gain stage will be provided in the post amplifier to establish the desired system gain. This adjustment will be made on initial installation and will not require further field adjustment.

2.8.3 Output Polarity

The post-amplifier output polarity will be negative going for positive or increasing IR modulation for compatibility with the MSS video processor.

2.8.4 Signal/Noise Data

Plots of signal/noise vs detector bias and detector operating temperature will be provided for each channel of the system.

3. SYSTEM ALTERNATIVE APPROACHES AND CONCEPTS

A number of candidate approaches were considered for the various functional areas of the LWS arrays during the first thirty days of this program. The basis for selection of the design concept given in Section 2 is discussed in Sections 3.1 and 3.2.

3.1 Detector Selection, Array Number 3

In the 2.3 to 4.63 μm wavelengths required for array 3, the choice of detector materials reduces to two, in the photovoltaic mode; Indium Antimonide (InSb) or Mercury Cadium Telluride (HgCdTe). For photoconductive mode operation, the choice is between InSb, HgCdTe, PbSe, or PbS (for the shorter wavelength channels). However, of the two operational modes, photovoltaic offers at least an order of magnitude advantage in signal bandwidth and, potentially, a factor of $2^{1/2}$ advantage in detectivities. For this reason, the selection was limited to Photovoltaic InSb or HgCdTe. Ultimately, InSb appeared to be the proper choice for application in the LWS for the following reasons:

a. Channel 14, the largest detector, requires a sensitive area of 0.102 by 0.55 inches. This is relatively large for presently available HgCdTe detector materials due to the number of dislocations which would occur in the sensitive area. At this time, starting material with dislocation densities of the order of 1,000/cm^2 can be procured. Although it is probably possible to obtain HgCdTe material with an acceptably low number of dislocations (100/cm^2), the yield would be too low to make the attempt economically feasible in the near term. InSb starting material, however, is routinely manufactured with dislocation densities of the order of 100/cm^2 or less.

b. InSb detectors are manufactured by a number of suppliers including Aerojet and are available in the sizes required for the LWS system. They can meet the detectivity (D^*) and bandwidth requirements and would probably be an order of magnitude less expensive than the HgCdTe detectors. Even if the dislocation problem associated with the HgCdTe could be overcome, the large cost differential favors selection of InSb detectors.

For the above reasons, Aerojet considered photovoltaic InSb detectors the unique best choice for meeting the performance requirements of the system in a timely manner and at a reasonable cost. It is reasonable to assume that other detectors will become available in the future which may have performance characteristics equal to or superior to the InSb. However, practical considerations of cost and schedule dictated the selection of InSb which is available now and which will fulfill the specific requirements of this application.

3.2 Detector Selection, Array Number 4

For the longer wavelength detectors of Array 4 (6.5 to 12.75 μm), a D^* of 4×10^{10} is required for wavelengths from 6.5 through 11.50 μm and 4.5×10^{10} for the detector operating at a center wavelength of 12.50 μm. Initial selection of detector materials again involved a choice between photovoltaic and photoconductive types. In the case of these longer wavelength detectors, the photovoltaic type could not be seriously considered. The only available materials which could satisfy the detectivity requirements are PbSnTe and HgCdTe. PbSnTe detectors would have satisfactory performance, but in the present state of development they cannot be made in the large size required. Photovoltaic HgCdTe detectors of this size are impractical since a dislocation in the junction constitutes a short circuit and starting material of sufficiently low dislocation density is not currently available.

For operation in the photoconductive mode, only two materials merited investigation as possible choices; Ge:Hg and HgCdTe. The HgCdTe detector has several serious deficiencies which eliminated it as a candidate material for this application:

a. The resistance of the material is low (approximately 50 ohms per square). Since the bias voltage required for detector operation increases as the square of the dimension in order to maintain a constant responsivity, Joule heating becomes significant for detectors larger than approximately 0.020 x 0.020 inch. This heating increases as the fourth power of the detector size. Thus, reduction of the applied voltage in order to control heating results in loss of responsivity and D^*.

b. Signal bandwidth is generally less than required for this application. While this may be corrected in theory by suitable lead compensation in the preamplifier, a serious practical difficultry arises in the case of low impedance detectors. Lead compensation has the effect of accentuating high frequency preamplifier noise. Where the margin of detector-noise-limited operation is small, as is usually the case for low impedance detectors, a penalty in D^* is attendant to lead-compensation.

c. Mercury doped germanium detectors can be fabricated in the required size, exhibiting the required performance characteristics, (i.e., D^* and bandwidth). The only disadvantage associated with the use of Ge:Hg is that operating temperatures of the order of $30^{\circ}K$ are required. The only system penalty for low temperature operation is one of cooler power, which is not an overriding consideration in this application.

3.3 Cooler Selection

Cooler selection was based on the selected detector material operating temperatures, reliability, field maintainability, commonality of units for arrays 3 and 4, vibration level, cost, and efficiency.

Table IV has been included in this report to show the different characteristics of the Stirling and Gifford-McMahon cycle machines at the two operating temperatures. The Gifford-McMahon machine manufactured by Cryogenic Technology, Inc. was selected for use with the LWS system. The major shortcomings of this device; larger power consumption, and greater weight are not significant for this particular program. The advantages of higher reliability (1000 hrs. MTBF), commonality of units for both arrays and with other NASA devices, relative absence of self-induced vibration, availability, and ease of maintenance were factors influencing the selection of the Gifford-McMahon type device. Selection of the manufacturer was limited to CTI, since this firm has emerged the victor in the cryogenic cooler competition. The principle competitor, Malaker is no longer manufacturing coolers.

To further simplify the cooler subsystem, the possibility of using a common compressor for both refrigerators was investigated. CTI advised that they had manufactured a compressor at one time with sufficient capacity to operate both arrays. This compressor was discontinued because of unacceptable

TABLE IV

Comparison of Cryogenic Coolers (Air Cooled)

for 77°K and 26°K Applications

CHARACTERISTIC	77 KELVIN		26 KELVIN	
	CTI CRYOGEM	CTI CRYODYNE	CTI CRYOGEM	CTI CRYODYNE
MODEL NUMBER	460081	0130	460081	0120
REFRIG. CAPACITY (WATTS)	12	7	1	1
TYPE OF CYCLE	STIRLING	GIFFORD-MCMAHON	STIRLING	GIFFORD-MCMAHON
COOL DOWN TIME (0 MASS) MIN.	~4	5.5	~ 10	10
AMBIENT TEMPERATURE (°F)	75	75	75	75
AMBIENT OPER RANGE (°F)	-65→131	-65→131	-65→131	-65→131
POWER REQUIRED (W)	350 - 400	40 + 850	350 - 400	40 + 850
POWER CHARACTERISTICS	208 v 3Ø400~	208 v 3Ø400~	208 v 3Ø400~	208 v 3Ø400~
WEIGHT (POUNDS)	12	4.2 + 22	12	5 + 22
DISPLACER SPEED (RPM)	1750	150	1750	150
APPROX. SIZE (TO COLD TIP) (IN)	5 x 5.6 x 11	5.5 x 3.9 x 7.9	3.5 x 5 x 11	5.5 x 5 x 10.6
	--	10.4 x 8 x 10	--	10.4 x 8 x 10
APPROX. TOTAL VOL (CU. IN)	72	170 + 830	72	320 + 830
MAINTENANCE INTERVAL (HOUR)				
- OVERALL (STIR) OR REFRIG (GM)	250 +	1000	250 +	1000
- COMPRESSOR	--	2000	--	2000
- ADSORBER	--	500	--	500
MTBF (ESTIMATE) (HOUR)	?	2000	?	2000
VIBRATION AT COLD HEAD	NOMINAL	LOW	NOMINAL	LOW
- APPROX. AMPLITUDE (MIL)	1.0	0.15	1.0	0.15
OPERATING ATTITUDE	ANY	ANY (REFRIG)	ANY	ANY (REFRIG)
	--	± 60° (COMP)	--	± 60° (COMP)

NOTES:

1. DATA BASED ON PUBLISHED OR VERBAL CLAIMS BY MANUFACTURERS
2. WHERE TWO SETS OF NUMBERS ARE GIVEN, FIRST IS FOR REFRIGERATOR UNIT, SECOND IS FOR COMPRESSOR UNIT (CRYODYNE GIFFORD MCMAHON MACHINES)

reliability, however. Another shortcoming of the single compressor concept would be the loss of data from both long-wavelength arrays in the event of compressor failure.

The thermal chugging discussed earlier is a minor deficiency in the Gifford-McMahon unit. However, the short-term temperature variations resulting from this phenomenon can be virtually eliminated using the special lead-tin alloy thermal capacitance. The cost of empirical determination of the required thickness is not considered significant and does not off-set the other advantages of the system.

Aerojet originally proposed the use of a single stage refrigerator unit for the 77°K temperature of array 3. However, discussions with CTI revealed that the two-stage refrigerator (Cryogem 0120), which is intended for 27°K operation can be used for both arrays by substitution of an inactive second stage. With this modification, the 77°K temperature required for array 3 can be obtained. This alteration will require slightly more heating of the focal-plane assembly from the active temperature controller to obtain stable 77°K operation, but the power consumption will not be excessive. In all other respects, the cooler is identical to the standard unit. The refrigerator can be readily converted back to full two-stage operation by substituting the standard second stage expander for the dummy stage. This can be accomplished in the field by removal of a single locking pin once the refrigerator is disassembled.

The Vuillemier refrigeration system is another type of machine which has been used for the cooling of infrared focal-plane assemblies. At this time, the Gifford-McMahon is considered superior because of the experimental nature of the Vuilleumier devices.

In the configuration selected, the CTI Cryogem Model 0120 weighs a total of 15.5 lbs., and requires 790 watts of 3 phase, 400 Hz aircraft power. As illustrated in Figure 4 the refrigerator section occupies a significantly smaller volume than the Malaker coolers presently used with arrays 3 and 4. A typical compressor section occupies an additional volume which is approximately 10.5" H by 8.75" W by 10.5" L. Since the compressor units can be located remotely from the refrigeration section (and thus out of the MSS array and optical system area), the extra volume is not considered detrimental.

3.4 Preamplifiers

Preamplifier selection and design characteristics were based on the signal characteristics of the selected detectors, the noise figure acceptable for this design, and the electrical crosstalk requirements of the multi-element arrays.

Four approaches to detector-preamplifier integration were considered. These approaches, their advantages and disadvantages, and the approach recommended for this program are summarized in the paragraphs below.

The completely integrated approach would require the preamplifiers to be situated on the focal plane, in close proximity to the detectors, and to operate at detector temperatures. This integrated design would completely eliminate problems of lead and cable capacitance and corresponding roll-off due to stray capacitance, but has several serious disadvantages. Power dissipation at the focal plane would increase the cooling load. The necessity for external bias connections in order to individually adjust detector bias would further increase the cooling load and made the design very vulnerable to vibration and microphonics. In addition, this type of design would require active components which are not available. Specifically, high gain-bandwidth operational amplifiers which operate at cryogenic temperatures are not standard items.

A conventional voltage amplifier, external to the Dewar and operating at ambient temperature offers the advantage of simplicity and compactness. The capacitance of the detector leads and external cables, however, would make it impossible to achieve the required detector-preamplifier performance at the specified higher frequencies. ($\pm$ 0.5 db to 250 KHz).

A current-mode or "current feedback" amplifier, external to the Dewar and operating at ambient temperature, could be used to overcome part of the problem encountered with the external voltage amplifier. The cable shields could be driven to compensate for cable capacitance but the capacitance of the leads within the Dewar would still be a potential source of RC roll-off and microphonic pick-up. The additional complexity of the current mode amplifier, when coupled with the additional complexity required in the focal plane to minimize external/cooler induced microphonic noise, makes this

approach only marginally attractive.

The approach developed provides for impedance reduction within the Dewar; and further signal conditioning and amplification to the desired output levels external to the Dewar. Following the decision to incorporate a source-follower preamplifier stage on the focal plane assembly, both voltage mode and current mode (transimpedance) amplifiers were considered. This assumes that the source impedance provided by the parallel combination of detector and load is maintained below 50 Kohms. Both types of preamplifier were investigated for the LWS, and the transimpedance type was selected based on superior performance with regard to microphonics and electrical crosstalk.

Consideration was given to the advantages of packaging the operational amplifiers as well as the source-followers within the focal-plane assembly, but the concept was rejected. No benefit would be gained with operation in the evacuated space, since the amplifiers should be maintained at approximately ambient temperature anyway, and lead length is not critical following the impedance reduction stage. Placement of the amplifiers within the evacuated space could result in significant outgassing from the electronic components.

The preamplifier circuit design and component selection is presented schematically on Figures 6 and 7 for arrays 3 and 4 respectively. The design was developed from the following considerations:

a. Detector parameters, viz., noise, capacitance, resistance, bias requirement (offset voltage)

b. Frequency response

c. Buffering requirements (load resistor and source follower at cryogenic temperature)

d. System bandwidth design goal of $\pm$ 0.5 db from 0.05 Hz to 250 KHz.

Current-mode feedback amplifiers were selected to (1) provide the flat frequency response within $\pm$ 0.5 db to 250 KHz, (2) insure essentially detector-noise-limited performance, and (3) allow for flexibility in selecting a detector load resistor and adjusting detector bias (amplifier offset).

Also, a FET buffer stage (source follower) was added between the amplifier and detector load resistor for the following reasons:

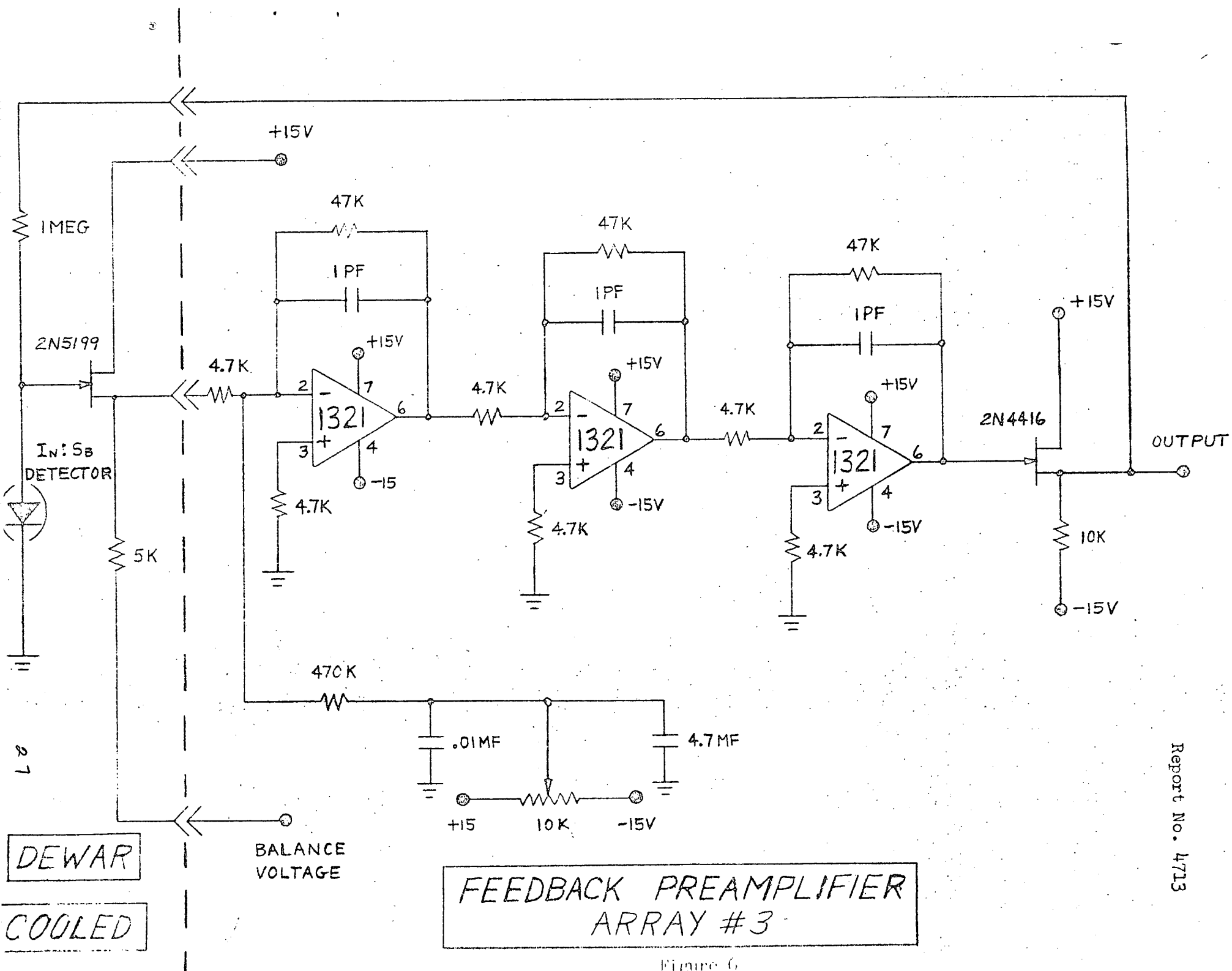
+15V
47K
1MEG
1PF
2N5199
4.7K
+15V
2
7
1321
6
3
4
-15
4.7K
47K
1PF
+15V
4.7K
2
7
1321
6
3
4
-15V
4.7K
47K
1PF
+15V
4.7K
2
7
1321
6
3
4
-15V
4.7K
2N4416
+15V
OUTPUT
10K
-15V
IN: SB DETECTOR
5K
470K
.01MF
4.7MF
+15
10K
-15V
BALANCE VOLTAGE
DEWAR
COOLED
FEEDBACK PREAMPLIFIER ARRAY #3

Figure 6

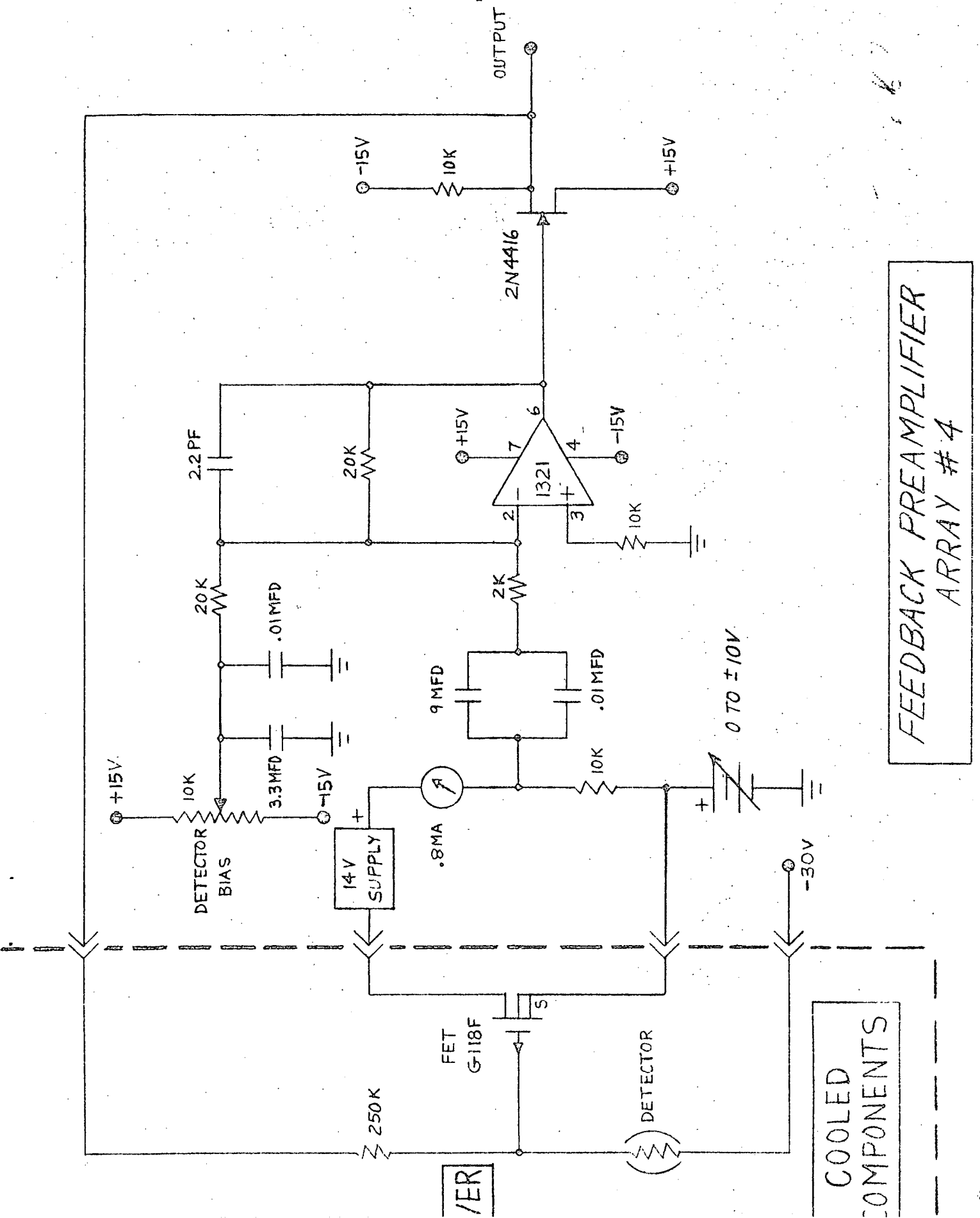
OUTPUT
-15V
10K
+15V
2N4416
2.2PF
20K
+15V
7
6
4
-15V
1321
2
3
10K
20K
.01MFD
2K
9 MFD
.01MFD
0 TO ±10V
+15V
10K
3.3MFD
-15V
DETECTOR BIAS
14V SUPPLY
.8MA
10K
-30V
FET G118F
S
250K
DETECTOR
FEEDBACK PREAMPLIFIER ARRAY #4
COOLED COMPONENTS

Figure 7

a. Output impedance (impedance presented to the amplifier) becomes independent of detector and load resistance.

b. Output impedance is less than 1 Kohm minimizing amplifier noise restrictions.

c. Essentially detector noise-limited performance is insured for the InSb detector (see noise analysis, Appendix B).

Since FETs can be cryogenically cooled, it is possible to locate the source-follower junction physically close to the detector. This technique minimizes the effects of capacitive loading due to cable length, microphonic pickup, and random noise effects. It also permits remote location of the preamplifier/post amplifier electronic packages within the MSS. Cable length of up to six feet will not impair the system performance.

Figure 7 is the schematic diagram of array No. 4 preamplifier. The preamplifier consists basically of an operational amplifier biased for a gain of 10 and a detector bias control. A breadboard of this preamplifier was tested against a simulated detector/buffer composed of a 250 Kohm load resistor, 250 Kohm resistor in place of the detector and an M511 MOSFET (M511 and G118 differ only in mechanical packaging). Results of these frequency-response and noise measurements are shown as Figures 8, 9, and 10. Voltage-mode data was measured at the source-follower output (dewar) with no amplifier or feedback provided. Current-mode data was measured at the preamplifier output. Pertinent features of the data are as follows:

a. Flat frequency response is increased from 100 KHz to 1 MHz from voltage mode to current mode.

b. Current-mode noise is less than 200 $nv/Hz^{\frac{1}{2}}$ at 1 KHz which is several orders of magnitude less than that expected from the GeHg detector.

Figures 11, 12, and 13 show corresponding data taken from the demonstration detector and preamplifier tested in simulation. Results indicate close agreement between simulation and real detector noise and frequency response. The irregular droop in current-mode frequency response is also present in voltage mode and is clearly a function of the specific detector physics. This can be corrected easily by a compensation network in the feedback loop. A deviation of less than 0.5 db in frequency response will probably require an active

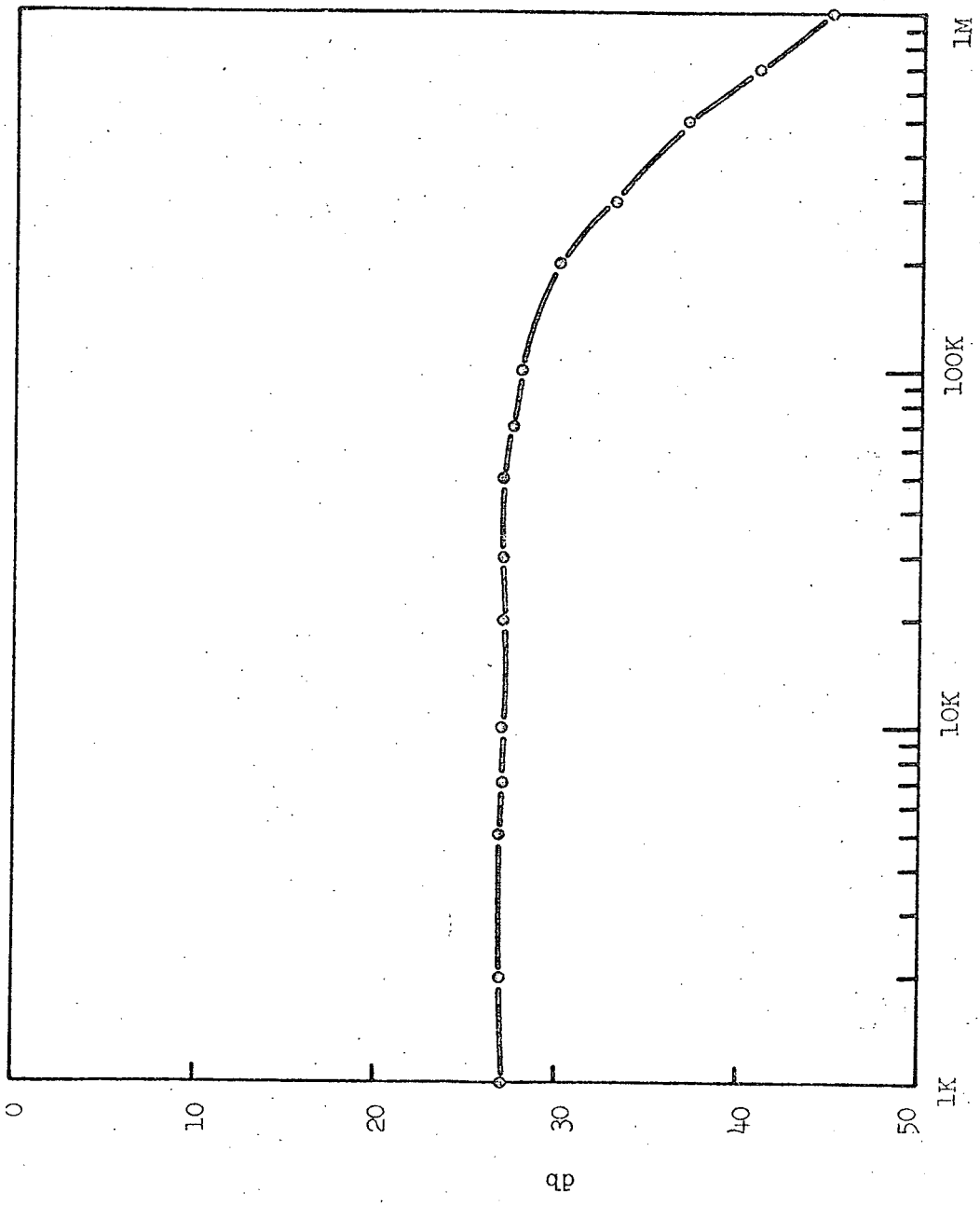

Figure 8. - ARRAY NO. 4 SIMULATED DETECTOR SIGNAL FREQUENCY RESPONSE, VOLTAGE MODE
ODB = 0.75 V

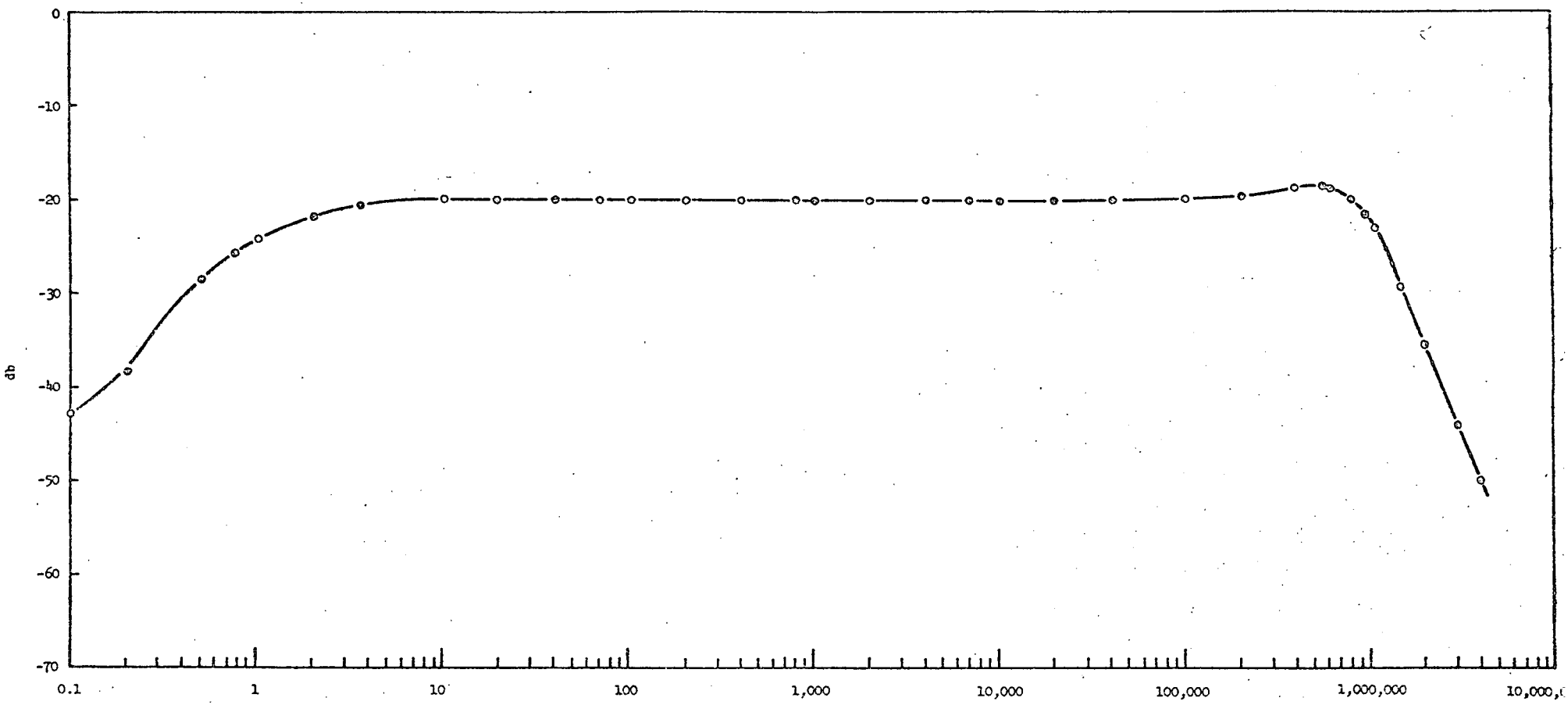

Figure 9. - ARRAY NO. 4 SIGNAL FREQUENCY RESPONSE WITH BREADBOARD AMPLIFIER AND SIMULATED DETECTOR
T = 300°K, 0.75V = 0 db

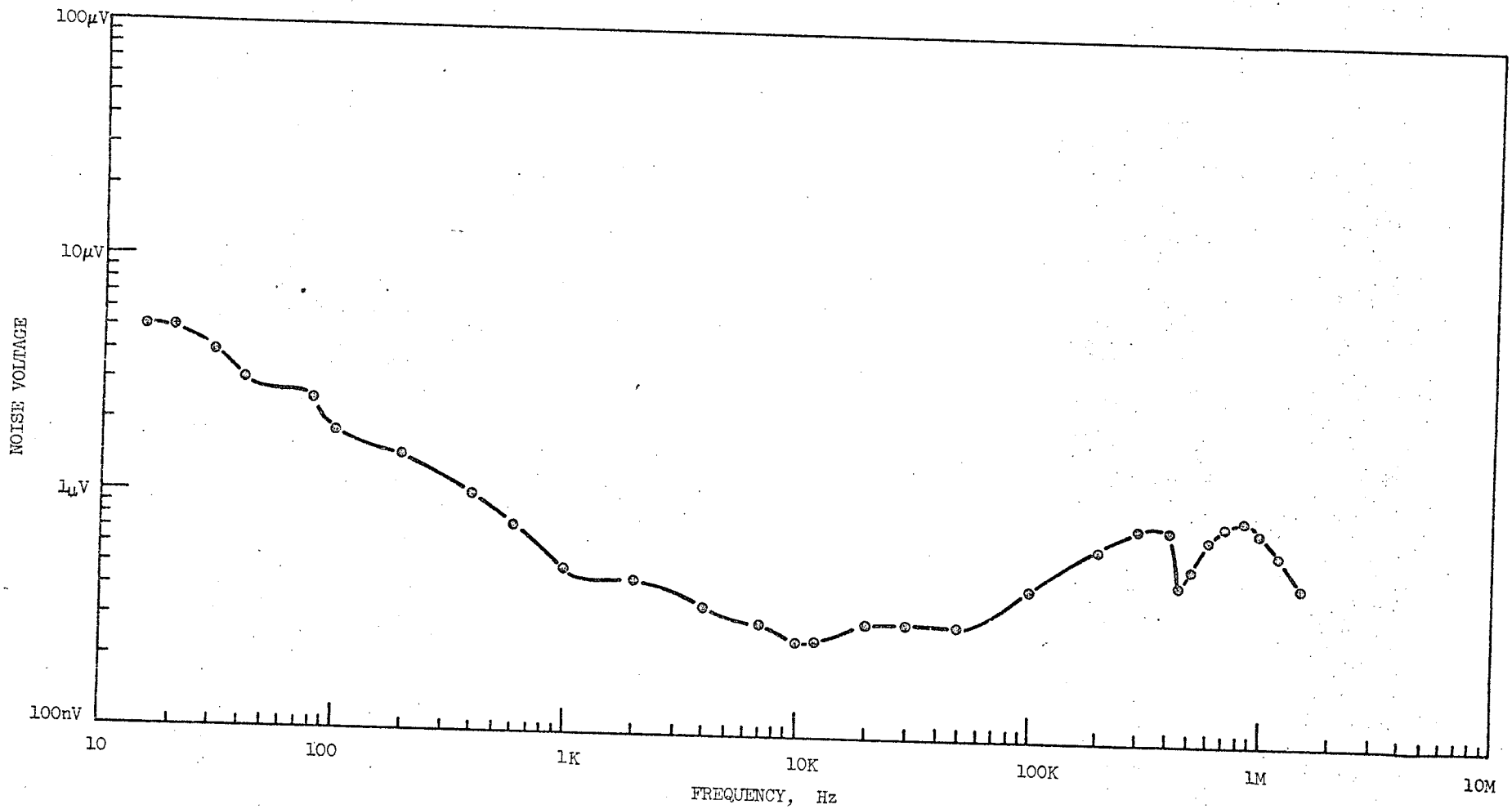

Figure 10. - NOISE, CURRENT MODE, BREADBOARDED ARRAY NO. 4 PREAMPLIFIER AND SIMULATED DETECTOR/BUFFER

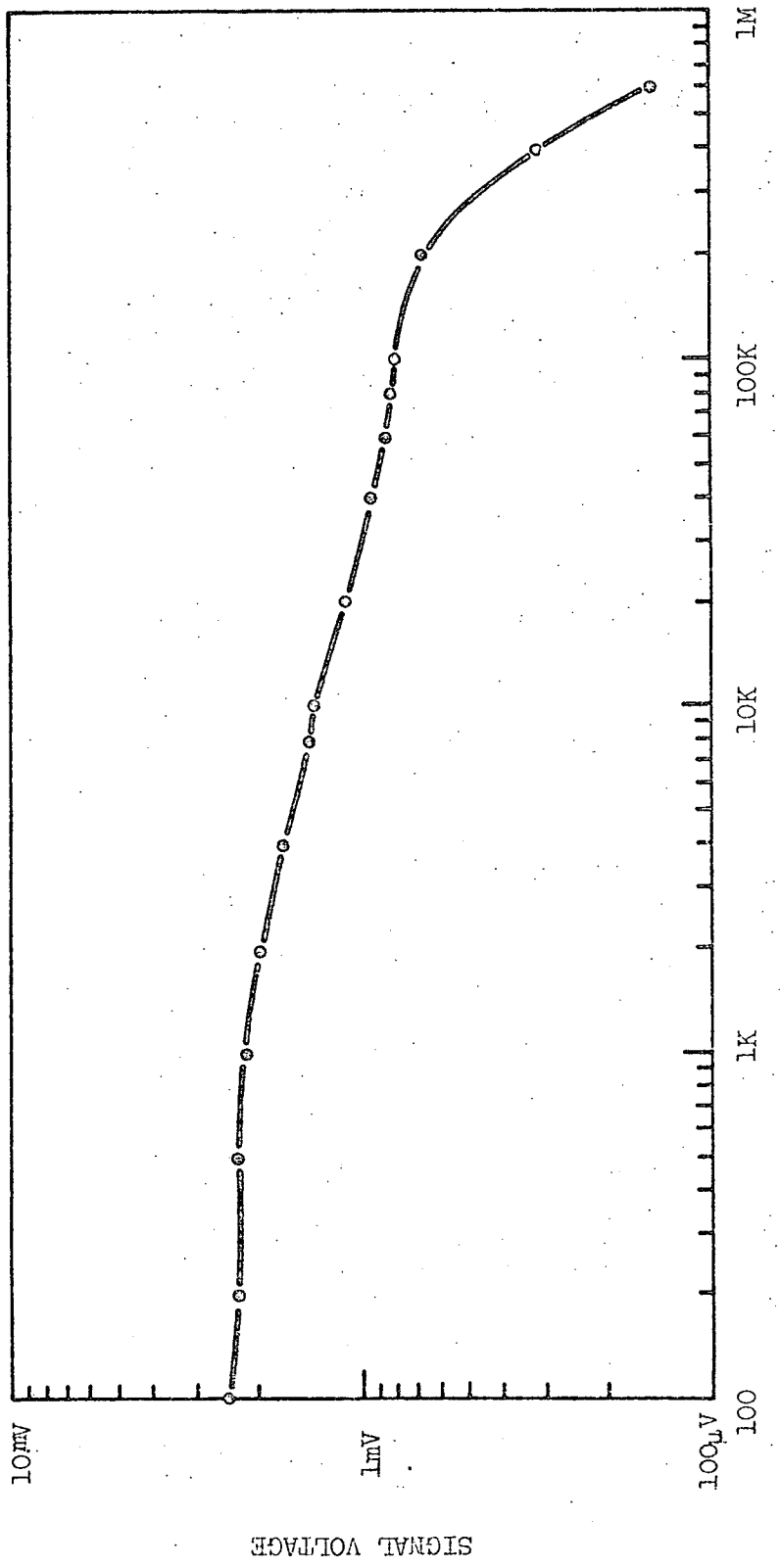

Figure 11. - SIGNAL RESPONSE, VOLTAGE MODE, DETECTOR AND BUFFER BREADBOARD, ARRAY NO. 4 (COOLED AT 28°K)

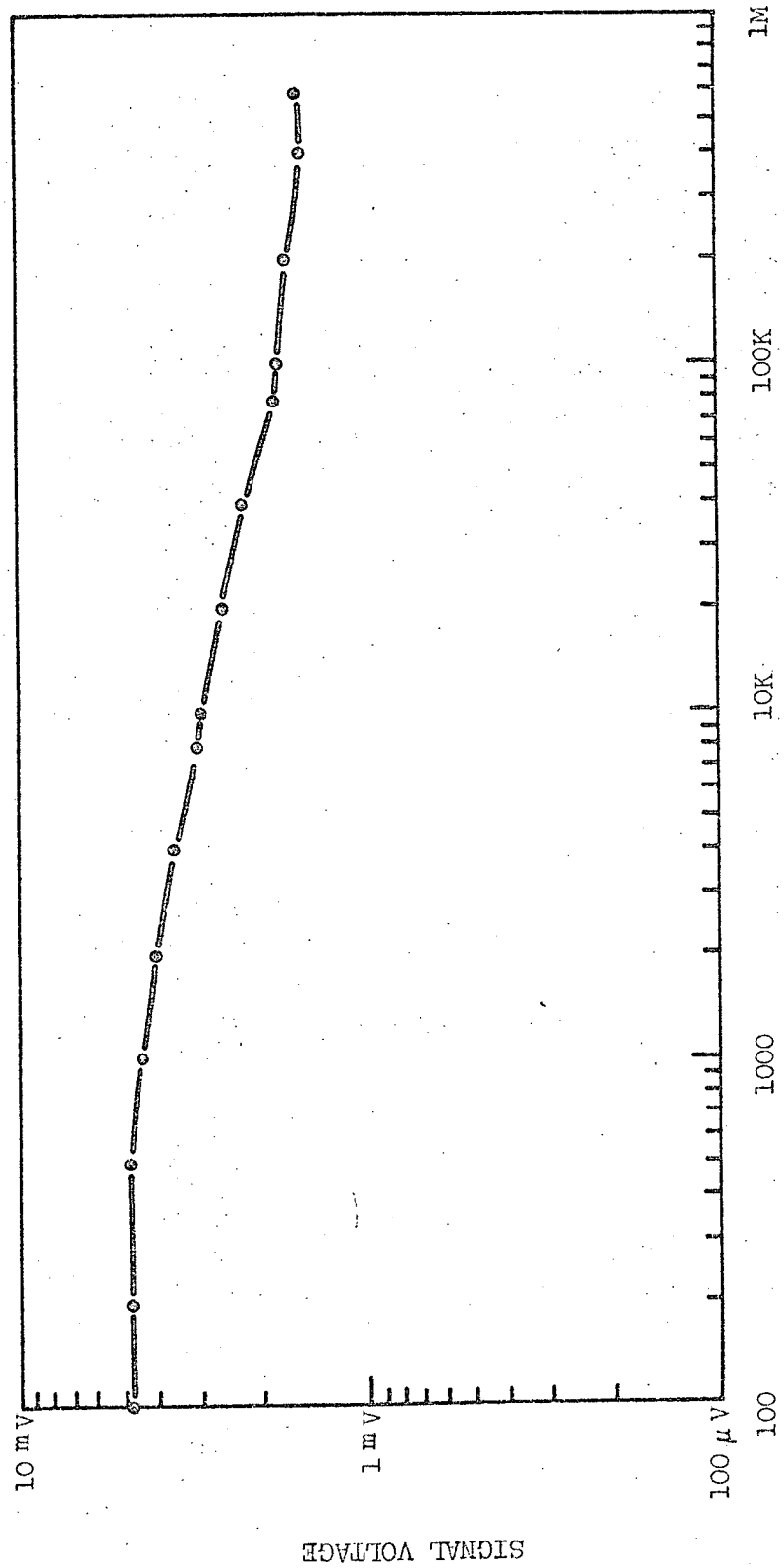

Figure 12. - SIGNAL RESPONSE: DETECTOR, BUFFER, AND PREAMPLIFIER BREADBOARD (DETECTOR AND BUFFER COOLED TO 28°K)

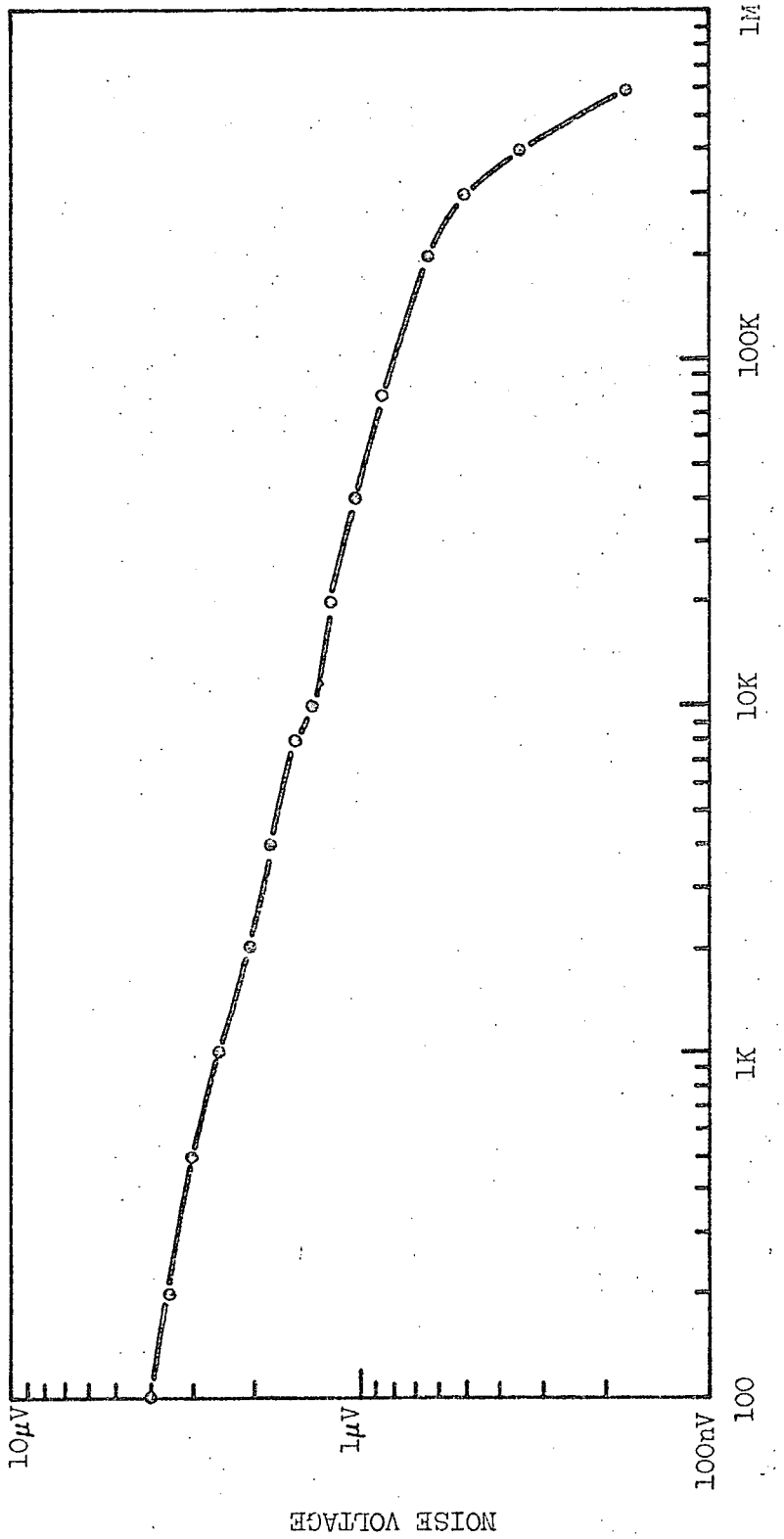

Figure 13. - NOISE, VOLTAGE MODE DETECTOR AND BUFFER BREADBOARD, ARRAY NO. 4
(COOLED TO 28°K, Δf = 10 Hz)

compensation network (multiple poles and zeros). Because each detector will require different compensations, selection of the networks will be accomplished empirically.

Analysis of the array No. 4 preamplifier noise characteristics indicates that the same amplifier design will not render the system detector-noise-limited when used with the photovoltaic InSb detectors. Analysis of the InSb amplifier/detector combination indicates that R_L (load resistor) must be 1 megohm minimum and that a low-noise JFET (e.g., 2N5199) buffer the detector/load resistor.

Voltage-mode performance data indicated that an amplifier stage properly biased will yield a detector-noise-dominated system. The large ratio of load resistor to detector resistance (≈ 4) and detector capacitance of approximately 1400 pf (worst case) indicates a required gain of approximately 1000. This can be achieved with three operational amplifier stages and provide adequate bandwidth margin.

Frequency-response compensation will be provided with peaking networks similar to those planned for the array No. 4 amplifiers.

3.5 Post Amplifier

The post-amplifier circuit diagram is shown as Figure 14. The unit is composed of three major blocks. These blocks and their function are:

(1) Input buffer (NH0002) - isolates driving circuit (feedback pre-amplifier) from clamp circuit.

(2) Amplifier and clamp (1321 operational amplifier plus clamp-driving circuitry) - provides a gain (schematic shows 20) and interfaces clamp/restore level and timing to the system.

(3) Output driver (NH0002) - provides current amplification to drive 50 ohm cable. Figures 15 and 16 show frequency response and clamp-circuit performance respectively.

3.6 Mechanical Features of the Design

The selected design is illustrated in Figures 1, 2, and 3. Special consideration during the design effort was allocated to incorporating the following features:

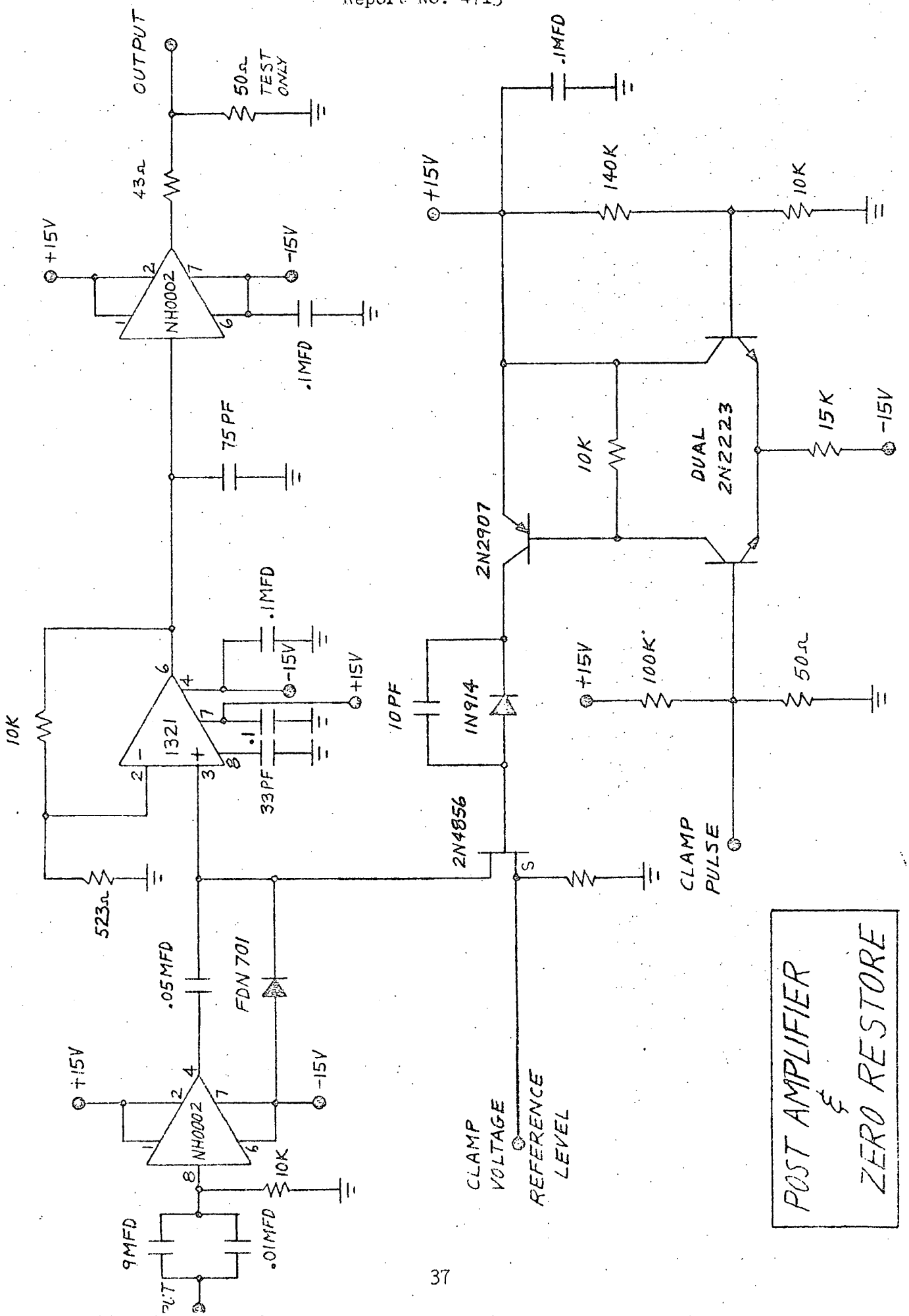
POST AMPLIFIER
&
ZERO RESTORE
OUTPUT
50Ω TEST ONLY
43Ω
+15V
-15V
NH0002
.1MFD
75PF
10K
1321
33PF
523Ω
.05MFD
FDN 701
9MFD
.01MFD
CLAMP VOLTAGE
REFERENCE LEVEL
10PF
IN914
2N4856
2N2907
DUAL 2N2223
140K
15K
100K
CLAMP PULSE

Figure 14

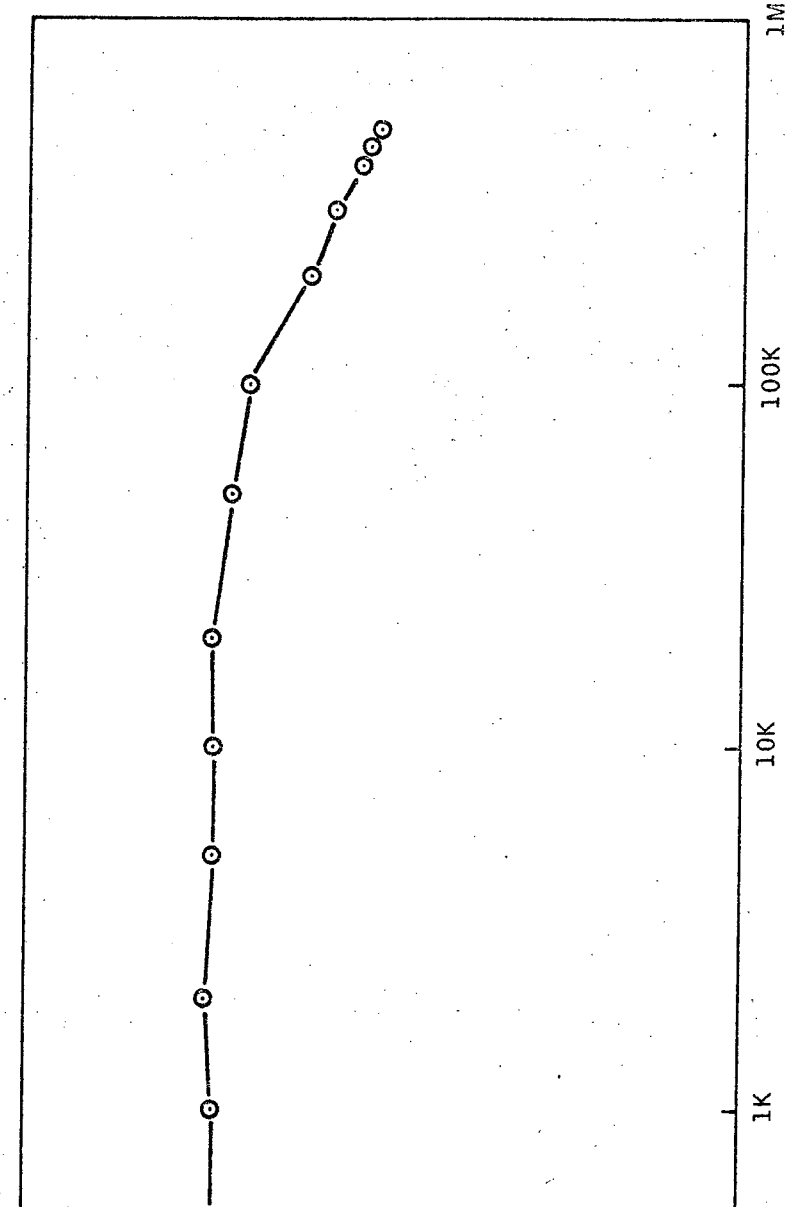

Figure 15. - Post Amplifier Frequency Response

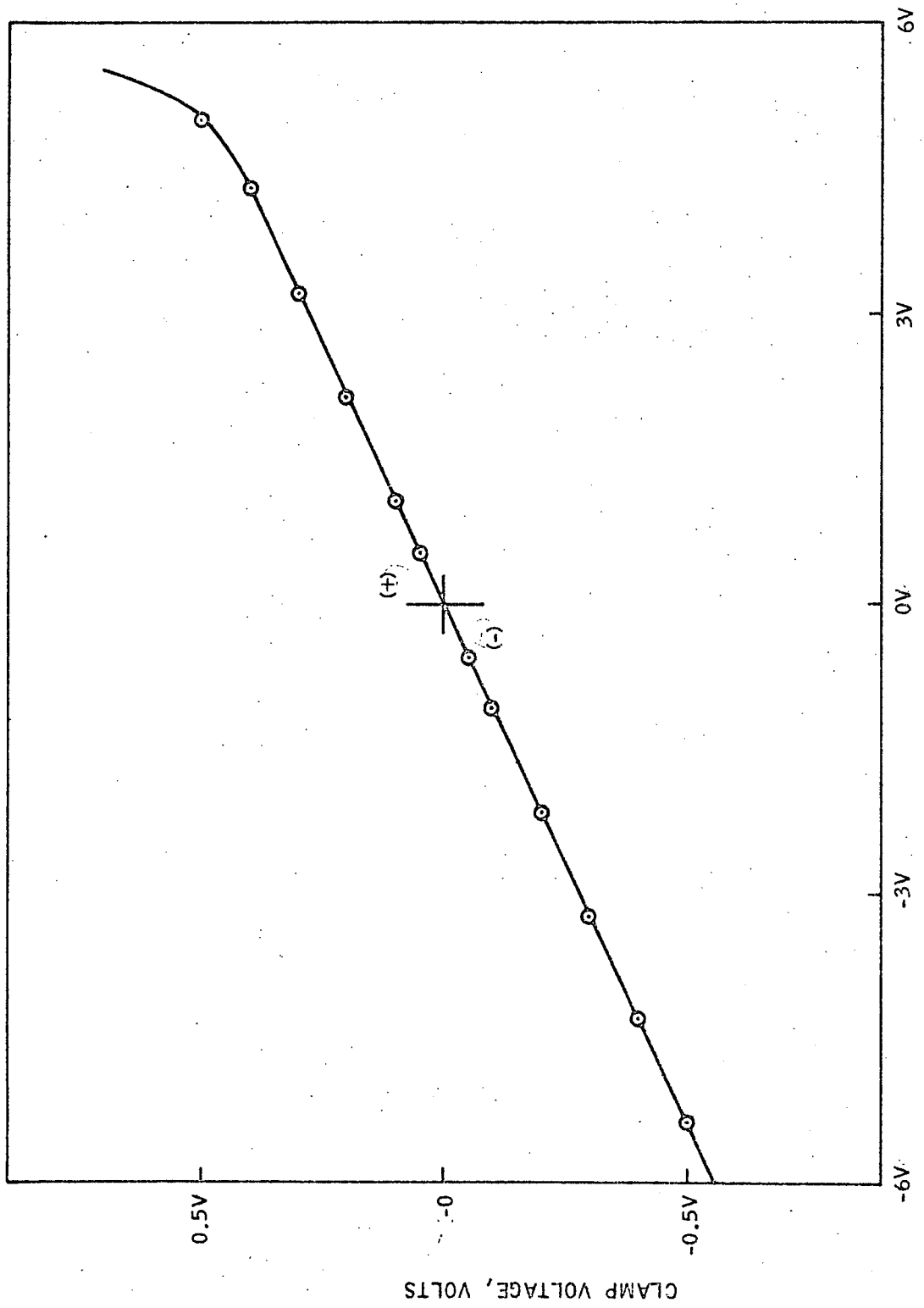

Figure 16. - Effect Of Clamp Voltage On Output Offset Level
Post Amplifier

a. Compatibility with the existing Multi-Spectral Scanner hardware.
b. Positive alignment adjustments with provision for locking after adjustment.
c. Rigidity of the housing assembly in order to maintain optical alignment and to reduce vibrational inputs to the detector assembly.
d. Ease of system evacuation and vacuum integrity of the assembly.
e. Field maintainability and commonality of components.
f. Selection of construction materials with minimal outgassing characteristics.

Aerojet believes that the above goals have been achieved with the optimum design depicted on Figures 1, 2, and 3.

4. CONCLUSIONS

The final design outlined in this report describes the recommended approaches for the fabrication of arrays 3 and 4 following extensive investigation, analysis, and trade-off studies. Aerojet believes that this approach incorporates all of the features required by the Multi-spectral Scanner System and that the desired performance can be provided with little technical risk.

The cost of the arrays and auxilliary devices will be very competitive with other approaches and they can be fabricated and delivered in a relatively short time span (approximately 4 months). Arrays 3 and 4 can be incorporated into the existing multi-spectral scanner system with a minimum of difficulty and will provide reliable performance within specification requirements.

APPENDIX A

LWS Breadboard Test Demonstration

10 DESIGN/PROTOTYPE TESTING

AESC/NASA tested breadboard type hardware on Monday, the 29th of January 1973, in conformance with the LWS Design Replacement Study Statement of Work (Section B. Design/Prototype Testing). The breadboard hardware, developed by AESC during the design replacement study, was tested to verify that it met the general performance requirements stated under section 2.3...Requirements.

10.1 Test Equipment and Conditions

10.1.1 Test Equipment

A functional block diagram of the test equipment utilized during the performance testing of the breadboard hardware is shown in Figure A-1. The equipment utilized for the breadboard testing was chosen for its ability to provide, in the majority of cases, a quick and directly observable verification of a "representative" channel's performance.

10.1.2 Test Conditions

The test conditions for the two representative channels of array 3 and 4 were in accordance with the following:

a. GE:Hg Channel (equivalent to channel #20)

- System Bandwidth: 0.01 → 250^{+} KHz
- Dewar Window: KRS-5 (≈70% transmission)
- Detector Operating Temperature: 28 K ± 0.5 K
- Blackbody Temperature: 500 K
- Ambient Temperature: ≈300 K
- Blackbody Aperture: 0.508 cm

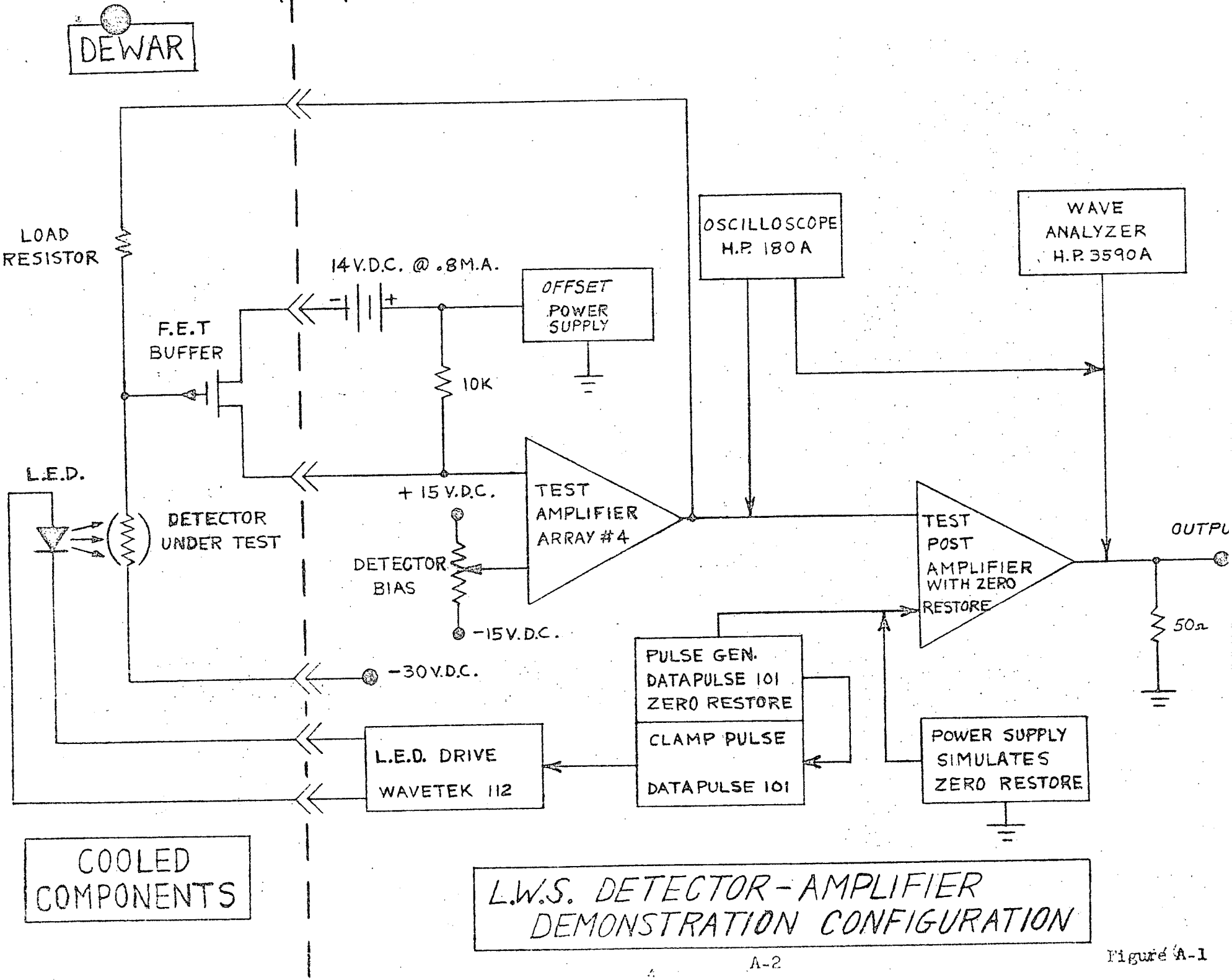

L.W.S. DETECTOR-AMPLIFIER DEMONSTRATION CONFIGURATION

Figure A-1

- Blackbody to Detector Distance: 25.4 cm
- Detector FOV: Equivalent to f/1.4
- Cold Spectral Filter: Same as filter in channel #20, MFSP-4 and specification
- InSb Light Emitting Diode (in cavity with detector)
- Cooled M-511 MOSFET (operating at detector temperature and wired up as source follower)
- Cooled 250 K Ω Detector Load Resistor
- Blackbody Chopper Frequency: 1000 Hz
- Current Mode Gain: 1/2
- Post Amplifier Gain: 20
- Net Amplifier Channel Gain: 10
- Detector Bias: +15V

b. <u>InSb Channel</u> (equivalent to channel #15, see Section 10.2 for explanation of prototype hardware)

- System Bandwidth: 0.03 Hz → 300 KHz (Princeton Applied Research Model #113 Amplifier)
- Dewar Window: KRS-5
- Detector Operating Temperature: 500 K
- Blackbody Temperature: 77 K ± 0.5 K
- Ambient Temperature: ≈300 K
- Blackbody Aperture: 0.508 cm
- Blackbody to Detector Distance: 25.4 cm
- Detector Field of View: Cold shielded to provide background photon flux density equivalent to that expected in channel #15 when cold filtered with f/1.4 cold shield
- Cooled 2N5199 JFET (operating at detector temperature and wired up as source follower)
- Cooled 330 K Ω Detector Load Resistor
- Blackbody Chopping Frequency: 1000 Hz
- Detector Bias: ≈ -160 mv

10.2 Prototype Hardware

The hardware tested for performance verification is shown functionally in Figure A-2. Channels #20 (Ge:Hg) and #15 (InSb) were selected by AESC for breadboard testing because they were felt to be the best representative detector channels of the two arrays. Since the "current feed back" and "post amp...zero restore" portions of the Ge:Hg channel and the InSb channel are nearly identical (difference of gain in the feedback loops) it was felt appropriate to only test/verify the end-to-end performance of one complete channel (the Ge:Hg channel) and test for D^*/spectral response the performance of the cryogenically "buffered" InSb channel.

10.3 Testing Requirements

The tests required to be performed on the breadboard hardware are listed below. Tests a, b, and e were directly observed/verified with the test equipment. The conformance of the breadboard equipments to the remaining requirements is shown in Section 10.4 using extrapolation and the presentation of data generated prior to and/or during the test period.

a. Detectivity (D^*)--500 K blackbody, 1000 Hz
b. Responsivity vs frequency--1000 to 250,000
c. Spectral response of the detector material
d. Wideband noise measurements
e. Preamplifier "zero restore signal" performance
f. Detector, preamplifier responsivity--output signal level.

10.4 Test Results

The results of the tests conducted by AESC/NASA are shown below in summary form along with supporting test rationale. All the test data were recorded on AESC engineering work sheets and copies have been supplied to Mr. J. Kessel (NASA) for his review and approval prior to its inclusion in the final document package.

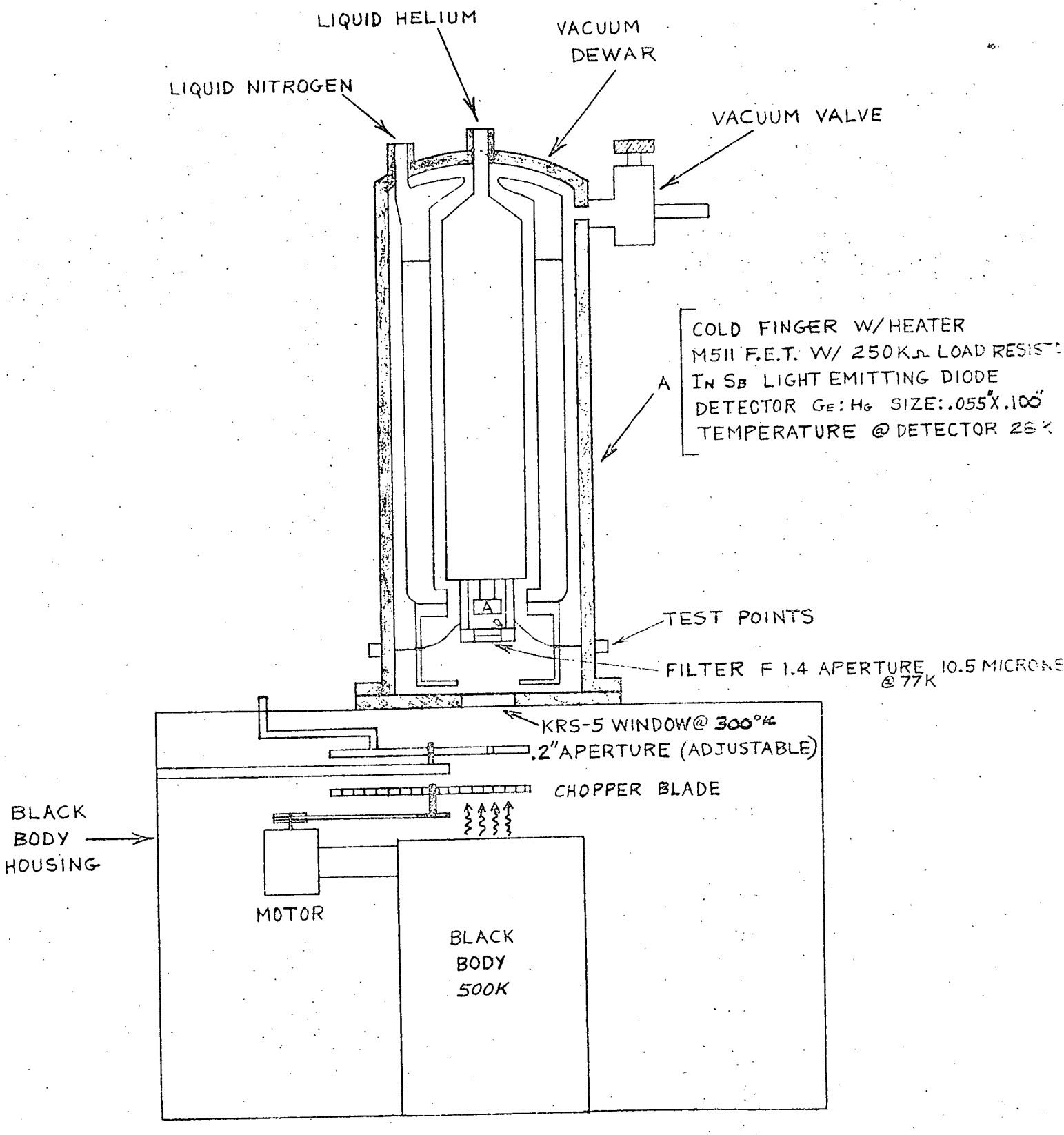

DETECTOR TEST STAND

Figure A-2

2. Responsivity vs Frequency

The wave analyzer employed for this test (310A) would not permit accurate readings below 1 KHz. It was, therefore decided to run the detector channel signal level vs frequency from 1 KHz to 400 KHz instead of the original requirement of 200 Hz.

Frequency	Signal Level* (mv)
1 KHz	5.0
5 KHz	4.3
10 KHz	3.8
50 KHz	2.8
100 KHz	2.55
200 KHz	2.6
250 KHz	2.85
300 KHz	2.90
350 KHz	2.70
400 KHz	2.50

Although this test indicated that the detectors signal level is approximately 6 db down at 400 KHz, it was also noted that noise vs frequency behaved in a similar manner. Consequently, a simple boost in the high-frequency response of the current mode amplifier can bring the detector's signal and noise up to the required level (± 1 db to 250 KHz). It should be further noted that each detector (due to its photoconductive properties) will require its own unique peaking in order to satisfy the uniform responsivity requirements of this program and, as such, it was felt that preserving the signal-to-noise ratio of the detector to frequencies in excess of 250 KHz was more important than the demonstration of a flat signal frequency response which will necessarily have to be adjusted after the final fabrication/selection of the detectors for array 3 and 4.

* Diode emitter used for this test since the blackbody chopper was not capable of frequency in excess of 5 KHz.

3. Spectral Response

See attached spectral response for the Ge:Hg detector.

4. Wideband Noise Measurements

This measurement was inadvertently not taken. It was noted, however, by AESC/NASA that the detectors wideband noise (on-scope) was approximately a factor of 6 to 10 times the amplifiers noise and consequently, the channel was appropriately detector, not preamplifier noise limited.

5. Preamplifier "Zero Restore Signal" Performance

The preamplifier performance requirement was verified using the insertion of a dc voltage of adjustable level into the "clamp voltage" input of the post amplifier (see Figure 14) and noting that the detector signal's shape and relative amplitude (relative to dc clamp level) was preserved.

6. Detector, Preamplifier Responsivity--Output Signal Level

For the purpose of this test, a total channel gain of 10 was arbitrarily selected in order to demonstrate that gain can be introduced into the processing channel by way of the post amplifier without degrading the performance of the detector (increasing noise and/or reducing frequency response). This was verified during the performance testing of this channel.

It should be noted that the actual gain required for each channel is a function of the irradiance on the individual detectors as well as the responsivity of the individual detectors proper and consequently cannot be exactly specified until the detectors/buffer electronics have been integrated and characterized.

The delta photon flux at the individual detectors, provided by the multispectral scanner optics, is tabulated in Table A-I and was calculated utilizing the data provided by NASA, November 5, 1972. For

channel #20, for example, a change in target temperature of 20 K would give rise to a photon flux change at the detector of 3.98×10^{12} photons/sec. This change, when compared to the irradiance change generated by way of the chopped blackbody (a delta irradiance of 4.56×10^{-7} w/cm^2, or an equivalent $\Delta\phi$ = 1.69×10^{12} P/sec) which produced an output signal level of 10 mv (gain x 10) would indicate a gain of 42.5 is actually required for this channel in order to meet the 100-mv signal level change when a target, as viewed by the multispectral scanner, changes its temperature by 20 K.

TABLE A-I

Delta Photon Flux (Photon/sec) vs Channel
(Target $\Delta T = 20^{\circ}K$)

Channel No.	Photons/sec
13	2.66×10^{8}
14	1.22×10^{11}
15	2.04×10^{11}
16	2.53×10^{12}
17	1.33×10^{12}
18	1.48×10^{12}
19	1.11×10^{12}
20	3.98×10^{12}
21	3.80×10^{12}
22	4.35×10^{12}

For example:

$$\frac{100 \text{ mv}}{\frac{\Delta Q1 \times 10 \text{ mv}}{\Delta Q2}} = K = \text{additional gain required.}$$

where $\Delta Q1$ = irradiance change at the detector due to a 20 K target temperature change and multispectral scanners optics

$\Delta Q2$ = irradiance change generated via chopped 500 K blackbody

and $K = \text{additional gain required} = \frac{\Delta Q2(10)}{\Delta Q1} = \left(\frac{1.69 \times 10^{12}}{3.98 \times 10^{12}}\right) 10 = 4.25$

with the demonstrated gain of 10 and the additional gain of 4.25, the total system gain of tested channel would require an actual gain of 10 x 4.25 or 42.5.

b. Channel #15 (Equivalent) InSb

1. D^*--500 K Blackbody, 1000 Hz

Measured Signal = 7.2 mv

Measured Noise = 1.5×10^{-7} V (6 Hz bandwidth)

Signal-to-Noise Ratio = 4.8×10^4

$\therefore$ Since $D^*_{\lambda peak} = S/N \times \sqrt{\frac{\Delta f}{A_D}} \times \frac{1}{H_{RMS}} \times K$

and $$H_{RMS} = \frac{W_{fs} \times A_p \times M_f \times \text{Cos } \Theta \times T_w}{\pi D^2} \ (w/cm^2)$$

where

$D^*_{\lambda peak}$ = detectivity at the spectral peak

S = signal of the detector (volts)

N = noise of the detector (volts)

K = ratio of peak D^* to blackbody $D^* = 5.7$

A_D = area of the detector (cm^2)

A_p = area of the blackbody aperture (cm^2)

M_f = modulation factor

Θ = angle of detector's normal to blackbody normal

T_w = weighted transmission of the Dewar window (%/100)

D = distance between the detector and the blackbody (cm)

W_{fs} = blackbody output (effective)(w/cm^2)

$$H_{RMS} = \frac{(3.04 \times 10^{-1})(6.45 \times 10^{-2})\ \pi(1)(4.4 \times 10^{-1})(0.7)}{\pi \times 6.45 \times 10^2}$$

$$H_{RMS} = 9.36 \times 10^{-6} \ w/cm^2$$

and $\sqrt{\Delta f} = 2.55\ Hz^{1/2}$, $\sqrt{A_D} = 1.4 \times 10^{-1}$ cm

$$D^*_{\lambda peak} = \frac{(4.8 \times 10^4)(2.55)(5.7)}{(9.36 \times 10^{-6})(1.4 \times 10^{-1})} \quad \frac{1.225 \times 10^5 \times 5.7}{1.31 \times 10^{-6}}$$

$$= 9.35 \times 10^{10} \times 5.7$$

$$= 5.33 \times 10^{11}$$

Now since $D^*_\lambda = \frac{R_{\lambda peak} (D^*_{\lambda peak})}{R_\lambda}$

where D^*_λ is the detector's D^* at some arbitrary wavelength λ, and R_λ is the spectral response of the detector at that λ, we find:

$$D^*_{\lambda(4.62)} = \frac{(4.8)}{(4.62)} (D^*_{\lambda peak}) = (0.97)(D^*_{\lambda peak})$$

$= 5.17 \times 10^{11}$ which is in excess of the 3×10^{11} specified.

2. Responsivity vs Frequency

(See Section 10.2...Prototype Hardware on justification for omission.)

3. Spectral Response

See attached spectral response for InSb detector.

4. Wideband Noise Measurements

N/A (see Section 10.2)

5. Preamplifier "Zero Restore Signal" Performance

N/A (see Section 10.2)

6. Detector, Preamplifier Responsivity--Output Signal Level

Although not measured due to the conditions stated in Section 10.2, the gain required in this channel is 109 (assuming the detector utilized in the final system is equivalent to the detector tested in terms of responsivity, etc.).

For example:

$$\frac{100 \text{ mv}}{\frac{\Delta Q1}{\Delta Q2}} = \frac{100 \text{ mv}}{7.2} = K = \text{actual gain required} = \left(\frac{100}{7.2}\right)\left(\frac{\Delta Q2}{\Delta Q1}\right)$$

where $\Delta Q1$ and $\Delta Q2$ are same terms as for channel #20, Ge:Hg.

For $\Delta Q1 = 2.04 \times 10^{11}$ and $\Delta Q2 = 1.6 \times 10^{12}$ we get

$$K = \left(\frac{1.6 \times 10^{12}}{2.04 \times 10^{12}}\right)\left(\frac{100}{7.2}\right) = 109$$

APPENDIX B

Noise Analysis of Detector/Amplifier System for Array 3

The equivalent circuit of an InSb detector with its associated feedback preamplifier and noise sources is shown as Figure B-1. An analysis of this circuit for noise content follows.

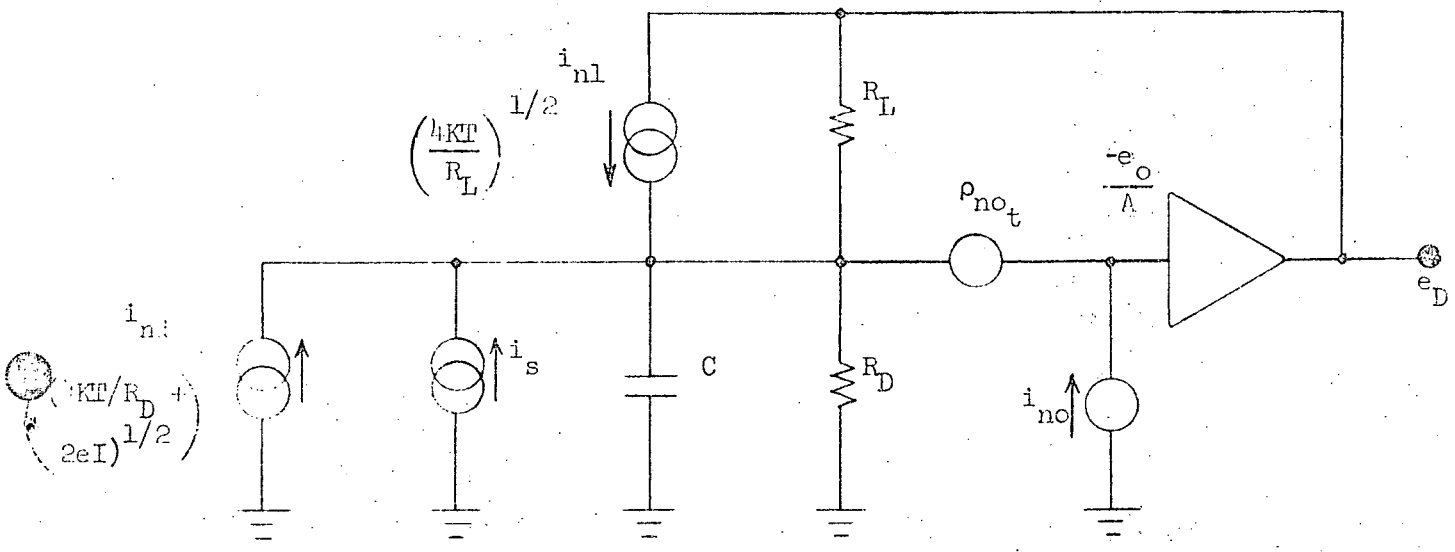

FIGURE B-1

Array 3 Detector/Preamplifier Noise Equivalent Circuit

i_{nl} - Johnson noise current of load resistor = $\left\{\frac{4KT}{R_L}\right\}$

i_{nd} - InSb detector noise = $\left[J_n^2 + S_n^2\right]^{1/2}$ $\left[\frac{4KT}{R_D} + 2eI\right]^{1/2}$

i_s - Signal current

i_{no} and e_{no} - noise current and noise voltage of amplifier (includes effects of input FET buffer)

Solving for noise components at e_o:

$$i_s = i_{nd} = e_{no} = i_{no} = 0$$

$$\frac{-e_{o1}}{A}\left(SC + \frac{1}{R_D}\right) + \left(\frac{-e_{o1}}{A} - e_{o1}\right)\frac{1}{R_L} - i_{n1} = 0$$

$$-e_{o_1}\left\{\left[\frac{1 + S\,R_D C}{AR_D}\right] + \left(1 + \frac{1}{A}\right)\frac{1}{R_L}\right\} = i_{nL}$$

Assuming $1 + \frac{1}{A} = 1$ and $\frac{1}{R_L} + \frac{1}{AR_D} = \frac{1}{R_L}$

$$e_{o1}\left\{\frac{SC}{A} + \frac{1}{R_L}\right\} = i_{nL}$$

$$e_{o1}^2 = \left\{\frac{i_{nL}}{\left[\frac{SC}{A} + \frac{1}{R_L}\right]}\right\}^2 = \frac{\frac{4KT}{R_L}}{\left(\frac{SC}{A} + \frac{1}{R_L}\right)^2} = \underline{\underline{\left\{\frac{4KTR_L}{\left(1 + S\frac{R_L C}{A}\right)^2}\right\}}}$$

$$i_s = i_{nL} = e_{no} = i_{no} = 0 \qquad i_{nd} \neq 0$$

$$\frac{-e_{o2}}{A}\left(SC + \frac{1}{R_D}\right) + \left(\frac{-e_{o2}}{A} - e_{o_2}\right)\frac{1}{R_L} - i_{nD} = 0$$

$$-e_{o2}\left\{\frac{SC + \frac{1}{R_D}}{A} + \left(1 + \frac{1}{A}\right)\frac{1}{R_L}\right\} = i_{nD}$$

$$1 + \frac{1}{A} \simeq 1$$

$$\frac{1}{AR_D} + \frac{1}{R_L} \simeq \frac{1}{R_L}$$

$$e_{o2} = \frac{-i_{nD}}{1 + S\frac{C}{A} + \frac{1}{R_L}}$$

$$e_{o2}^2 = \frac{i_{nD}^2 R_L^2}{\left(1 + S\frac{R_L C}{A}\right)^2} = \left(\frac{4KT}{R_D} + 2eI\right) \frac{R_L^2}{\left(1 + S\frac{R_L C}{A}\right)^2}$$

$$i_s = i_{nL} = i_{nd} = i_{no} = 0 \qquad e_{no} \neq 0$$

$$- \left(e_{no} + \frac{e_{o3}}{A}\right) \left(SC + \frac{1}{R_D}\right) - \left(e_{no} + \frac{e_{o3}}{A} + e_{o3}\right) \frac{1}{R_L} = 0$$

$$-e_{no}\left(SC + \frac{1}{F_D} + \frac{1}{R_L}\right) - e_{o3}\left(\frac{SC + \frac{1}{RD}}{A} + \left(1 + \frac{1}{A}\right)\frac{1}{R_L}\right) = 0$$

Assuming $1 + \frac{1}{A} \cong 1$ and $\frac{1}{R_L} + \frac{1}{AR_D} \cong \frac{1}{R_L}$

$$e_{o3} = - \frac{e_{no} \frac{1}{R_p} (1 + S R_p C)}{\left(S\frac{C}{A} + \frac{1}{R_L}\right)}$$

---

where $\frac{1}{R_p} = \frac{1}{R_L} + \frac{1}{R_D}$

$$= -e_{no} \frac{R_L}{R_p} \left(\frac{1 + S R_p C}{1 + S \frac{R_L C}{A}} \right) = -e_{no} \frac{R_L (R_L + R_D)}{R_L R_D} \left(\frac{1 + S R_p C}{1 + S \frac{R_L C}{A}} \right)$$

$$= -e_{no} \left(1 + \frac{R_L}{R_D} \right) \left(\frac{1 + S R_p C}{1 + S \frac{R_L C}{A}} \right)$$

$$e_{o3}^2 \qquad e_{no}^2 \left(1 + \frac{R_L}{R_D} \right)^2 \qquad \frac{\left(1 + S R_p C \right)^2}{\left(1 + S \frac{R_L C}{A} \right)^2}$$

$$e_{no} = i_{nD} = i_{nL} = i_s = 0 \qquad i_{no} \neq 0$$

Note i_{no} is in parallel with i_{nd} for $e_{no} = 0$

Therefore i_{no} component same as i_{nd} component except i_{nd} replaced by i_{no}.

$$e_{o4}^2 = \frac{i_{no}^2 R_L^2}{\left(1 + S \frac{R_L C}{A} \right)^2}$$

Total noise out = e_{oT}

$e_{oT}^2 = e_{o1}^2 + e_{o2}^2 + e_{o3}^2 + e_{o4}^2$ as derived above

$$= \left(\frac{i_{nL} R_L}{1 + S \frac{R_L C}{A}} \right)^2 + \left(\frac{i_{nD} R_L}{1 + S \frac{R_L C}{A}} \right)^2 + \left[e_{no} \frac{\left(1 + \frac{R_L}{R_D} \right) \left(1 + S R_p C \right)}{\left(1 + S \frac{R_L C}{A} \right)} \right]^2$$

$$+ \left(\frac{i_{no} R_L}{1 + S \frac{R_L C}{A}} \right)^2$$

For

$S = 0$

$K = 1.38 \times 10^{-23}$

$T = 77^{\circ}K$

$R_D = 250\ K$

$e_{no} = 15\ nv/\sqrt{H} = 1.5 \times 10^{-8}$

$i_{no} = 10\ pa = 10^{-11}$

TABLE B-1

Amplifier Noise for Various Load Resistances Array 3

R_L \ e_o^2	e_{o1}^2	e_{o2}^2	e_{o3}^2	e_{o4}^2
1.0×10^3	4×10^{-18}	1.7×10^{-20}	2.25×10^{-16}	1.0×10^{-16}
1.0×10^4	4×10^{-17}	1.7×10^{-18}	2.25×10^{-16}	1.0×10^{-14}
1.0×10^5	4×10^{-16}	1.7×10^{-16}	4.4×10^{-16}	1.0×10^{-12}
2.5×10^5	1×10^{-15}	1.0×10^{-15}	9.0×10^{-16}	6.25×10^{-12}
1.0×10^6	4×10^{-15}	1.7×10^{-13}	5.6×10^{-15}	1.0×10^{-10}

Table B-1 lists the results of this analysis for various values of R_L (load resistor). The above analysis shows that components of the amplifiers must be carefully chosen to insure essentially detector noise limited operation. Analyzing Table B-1 shows that for an R_L of 1M ohm, detector noise dominates all terms except e_{o4}^2 which is the component due to amplifier noise equivalent current. This component can be reduced by (a) selecting an amplifier with lower noise current (the i_{no} of 10 pa is a worst-case number and is one to two orders magnitude higher than that of top grade low noise operational amplifiers), (b) buffer the detector/load resistor combination with a FET source follower. This

reduces the impedance the i_{no} noise component drives. This may increase amplifier noise equivalent voltage (e_{o3}) by 2 (maximum) but this is of little importance as this component is well below detector noise. Thus an essentially detector noise limited system is insured.

APPENDIX C

Noise Analysis of Detector/Amplifier for Array 4

The equivalent circuit for a Ge:Hg detector is:

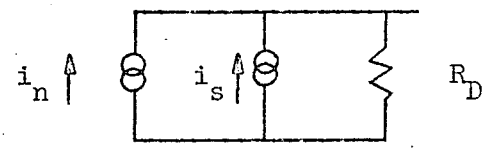

where R_D is approximately 250 KΩ

and i_n is determined as follows:

$$i_n^2 = 4\, e^2\, G^2\, A\, \eta\, \phi\, \Delta f$$

$$e = 1.6 \times 10^{-19}\ cm^{1/2}\ g^{1/2}$$

$$G = 1/2 \text{ to } 10$$

$$A = 1\ cm^2$$

$$\eta \cong 0.15 \text{ (worst case)}$$

$$\phi = \text{photon flux} = 3 \times 10^{16}\ \text{photons/cm}^2\text{/sec}$$

$$\frac{i_n^2}{\Delta f}\,(\min) = 4 \times (1.6 \times 10^{-19})^2\ 0.5 \times 0.15 \times 3 \times 10^{16}$$

$$\frac{i_n^2}{\Delta f} = 2 \times 2.56 \times 10^{-36} \times 0.45 \times 10^{16}$$

$$= 2.30 \times 10^{-20}$$

$$i_n\,(\min) = 1.5 \times 10^{-10} = 150\ \text{pa}/\sqrt{\text{Hz}}$$

This current into a 1KΩ resistance yields 150 nanovolts/$\sqrt{\text{Hz}}$ which is well above the noise-equivalent input of any of the amplifier configurations considered. Also, the input resistance of the detector load-resistor circuit is one to two orders of magnitude above the 1K considered above. Thus, for the Ge:Hg detector array, detector-noise-limited operation is insured by several orders of magnitude.